

A DIRECT APPROACH TO COMPUTING THE NON-INTERACTING KINETIC ENERGY FUNCTIONAL

DHARAMVEER KUMAR, AMUTHAN A. RAMABATHIRAN

ABSTRACT. The non-interacting kinetic energy functional, $T_{KS}(\rho)$, plays a fundamental role in Density Functional Theory (DFT), but its explicit form remains unknown for arbitrary N -representable densities. Although it can, in principle, be evaluated by solving a constrained optimization problem, the associated adjoint problem is not always well-posed; moreover, even when it is, the corresponding adjoint operator may be singular. To the best of our knowledge, none of the existing approaches in the literature precisely determines the non-interacting kinetic energy functional for a given N -representable electron density, ρ . In this work, we present a variational framework for computing an extension of $T_{KS}(\rho)$ using an exact trigonometric reparametrization of the density that eliminates the need for an adjoint equation. We present a proof-of-concept numerical validation of the variational principle for the special case of one-dimensional Kohn-Sham systems. Our method, however, is general and provides a systematic foundation for computing $T_{KS}(\rho)$ in higher dimensions too, paving the way for improved kinetic energy functionals in DFT.

1. INTRODUCTION

Density Functional Theory (DFT) provides a framework for describing many-electron quantum systems in terms of their electron density, ρ . In practice, most DFT calculations rely on the Kohn-Sham (KS) [KS65] formulation, which we refer to as KSDFT in the sequel. In KSDFT, fictitious orbitals are introduced to evaluate the ground-state electron density and energy, making the method computationally expensive. Orbital-Free Density Functional Theory (OFDFT), on the other hand, circumvents the need to compute fictitious orbitals by instead modeling the universal functional directly as a function of the electron density. This reduction in computational complexity makes OFDFT particularly appealing for modeling large-scale systems with thousands of atoms. A significant challenge in OFDFT is the explicit characterization of a major portion of the kinetic energy, called the non-interacting kinetic energy functional, denoted commonly as $T_{KS}(\rho)$, which can be accurately evaluated within KSDFT calculations. This article presents a rigorous analysis of an exact parametric approach to computing an extension of $T_{KS}(\rho)$ for a very large class of densities that include, in particular, KSDFT ground-state densities which corresponds to a given non-interacting potential.

(Dharamveer Kumar) DEPARTMENT OF AEROSPACE ENGINEERING, INDIAN INSTITUTE OF TECHNOLOGY BOMBAY, MUMBAI 400042, INDIA.

(Amuthan A. Ramabathiran) AEROSPACE ENGINEERING, CALIFORNIA POLYTECHNIC STATE UNIVERSITY, SAN LUIS OBISPO, CA 93407.

E-mail address: dharamveer_kumar@iitb.ac.in, aramabat@calpoly.edu.

Thomas-Fermi [Tho27] [Fer27] type models provide simple approximations of $T_{KS}(\rho)$, but they lack the necessary accuracy for many applications. More advanced formulations, such as the Wang-Govind-Carter (WGC) functionals [WGC98] rely on empirical parameterizations that can fail to capture key quantum mechanical features, limiting their transferability and accuracy, especially for inhomogeneous densities. These functionals introduce ad hoc gradient corrections that work well for bulk materials but struggle with systems exhibiting strong density variations, such as low-dimensional or defective systems. Despite these advancements, developing a universally accurate and computationally efficient kinetic energy functional remains an open problem in OFDFT, limiting its widespread adoption compared to KSDFT.

In recent years, there have been several attempts to leverage the flexibility of Machine Learning (ML) algorithms to learn approximations to kinetic energy functionals. ML-based kinetic energy functionals, however, often suffer from a lack of physical interpretability and limited generalizability beyond their training datasets. Most existing ML approaches derive kinetic energy densities indirectly from KSDFT calculations and are trained primarily on small datasets consisting of KSDFT ground-state densities; we note that ground-state densities constitute an *unknown* subset of N -representable densities. Although several efforts have been made to address these issues [SRH⁺12, MWH20, RWMT22], the training datasets for all these ML-based approaches still originate from KSDFT calculations, limiting their applicability to a truly orbital-free framework. Recently, [KLL⁺23] introduced a mathematically grounded operator learning framework that can, in principle, be used to learn complex functionals such as the non-interacting kinetic energy. However, training such models requires explicit evaluation of the energy for arbitrary electron densities.

To the best of our knowledge, there are no existing numerical methods to compute $T_{KS}(\rho)$ explicitly for arbitrary N -representable density. However, if such densities correspond to the ground state of a non-interacting potential, the Kohn-Sham inversion [HBL25] could be used. In KSDFT $T_{KS}(\rho)$ is implicitly computed starting from a potential via the KS orbitals obtained as part of the KSDFT calculations. This is also typically how the datasets used to train data-driven models for $T_{KS}(\rho)$ are generated. Thus, only a small subset of v -representable densities is sampled with conventional approaches. We present in this work a variational principle to compute an extension of the non-interacting kinetic energy functional for arbitrary N -representable densities, including those that are not v -representable, and validate our approach numerically using 1D KSDFT calculations. Our results offer a systematic approach for developing improved kinetic energy functionals and thus hold promise for developing OFDFT models with improved accuracy.

The article is organized as follows. In Section 2, we summarize certain relevant background material to set the stage for a variational formulation to evaluate an extension of the non-interacting kinetic energy functional. Throughout this work, we restrict attention to closed-shell systems. The variational principle that is the central thesis of this article is presented in Section 3. Representative numerical results validating our approach are presented in Section 4. In Section 5, we conclude with a discussion of some outstanding issues and the work to be

pursued in the future. Supplementary results and known propositions are presented in three appendices.

2. MATHEMATICAL BACKGROUND

We summarize in this section certain ideas from density functional theory, largely to fix the notation and set the context for the ensuing developments.

2.1. Background and Basic Definitions. The physical system studied in this work is a collection of N electrons interacting with each other via an interaction potential $w_{ee} : \mathbb{R}^d \rightarrow \mathbb{R}$ and subject to an external potential $v : \mathbb{R}^d \rightarrow \mathbb{R}$. We assume that w_{ee} is a non-negative even function and that v is negative. Following standard convention, we define $X = (\mathbb{R}^d \times \mathbb{Z}_q)^N$, with $q = 2$: any $x \in X$ can be written as $x = (r, \sigma) = (r_1, \sigma_1, r_2, \sigma_2, \dots, r_N, \sigma_N)$, where each $r_i \in \mathbb{R}^d$ and each $\sigma_i \in \mathbb{Z}_q$. We use the shorthand notation $\int_X f(x) dx$ for $\sum_{\sigma_1=1}^q \dots \sum_{\sigma_N=1}^q \int_{(\mathbb{R}^d)^N} f(r, \sigma) dr_1 \dots dr_N$, for any function f on X ; we will also use the notation \sum_q for $\sum_{\sigma_1=1}^q \dots \sum_{\sigma_N=1}^q$. We use the standard notation $\Lambda_1^N L^2(X)$ to represent the set of all square integrable antisymmetric wavefunctions. The following function spaces will be referenced frequently:

$$\begin{aligned} \mathcal{Q} &= \left\{ \psi \in \Lambda_1^N L^2(X) : \sum_{i=1}^N \int_X \|\nabla_{r_i} \psi\|^2 < \infty \right\}, \\ \mathcal{I}_N &= \left\{ \rho \in L^1(\mathbb{R}^d, \mathbb{R}^+) : \sqrt{\rho} \in H^1(\mathbb{R}^d), \int_{\mathbb{R}^d} \rho = N \right\}. \end{aligned} \quad (1)$$

Note that \mathcal{Q} collects all square integrable antisymmetric wavefunctions with finite kinetic energy. The set \mathcal{I}_N is an exact characterization of N -representable densities due to Lieb [Lie83]. The quadratic form associated with symmetric operator

$$H_v = \sum_{j=1}^N \left(\frac{-\Delta_{r_j}}{2} + v(r_j) \right) + \sum_{1 \leq j < k \leq N} w_{ee}(r_j - r_k) \quad (2)$$

is bounded from below and closed on \mathcal{Q} as a consequence of the Sobolev inequality when v and w_{ee} belong to $Y^d = L^p(\mathbb{R}^d; \mathbb{R}) + L^\infty(\mathbb{R}^d; \mathbb{R})$ [LLS23], with

$$p \begin{cases} = 1 & \text{when } d = 1, \\ > 1 & \text{when } d = 2, \\ = \frac{d}{2} & \text{when } d \geq 3. \end{cases}$$

Note that the Coulomb interaction in three dimensions belongs to Y^3 . The Friedrichs extension can be used to extend H_v to a self-adjoint operator. The ground state energy for a given potential v is defined as

$$E[v] := \inf_{\substack{\psi \in \mathcal{Q} \\ \int_X |\psi|^2 = 1}} (\psi, H_v \psi). \quad (3)$$

For a given wavefunction $\psi \in \mathcal{Q}$, we define the corresponding electron density $\rho_\psi : \mathbb{R}^d \rightarrow \mathbb{R}$ as

$$\rho_\psi(r) := N \sum_{\sigma} \int |\psi(r, \sigma_1, r_2, \sigma_2, \dots, r_N, \sigma_N)|^2 dr_2 dr_3 \dots dr_N. \quad (4)$$

It was established in [Lie83] that for $\rho \in \mathcal{I}_N$ there exists a $\psi \in \mathcal{Q}$ such that $\rho_\psi = \rho$. A density $\rho \in \mathcal{I}_N$ is said to be N -representable for this reason. In contrast, densities that correspond to the solution of the variational problem (3) are said to be v -representable, while those that correspond to the solution of (3) with $w_{ee} = 0$ are called non-interacting v -representable. Although a complete explicit description of the sets of v -representable and non-interacting v -representable densities is still unknown in full generality, in one dimension there has been notable progress toward characterizing large—in some cases complete—subsets of representable densities [SPR⁺24a, SPR⁺24b, Cor25]. These developments make the inverse method for the non-interacting kinetic energy feasible in 1D since it relies on being able to determine whether a density is non-interacting v -representable.

The central thesis of Hohenberg and Kohn’s density functional theory [HK64] is the restatement of the variational principle (3) in an exactly equivalent form in terms of the electron density. The constrained-search formulation due to Levy [Lev79] and Lieb [Lie83] exploits the fact that the set of all N -representable densities, \mathcal{I}_N , is known to rewrite the variational principle (3) as

$$E[v] = \inf_{\rho \in \mathcal{I}_N} \inf_{\substack{\psi \in \mathcal{Q} \\ \rho_\psi = \rho}} (\psi, H_v \psi). \quad (5)$$

Defining the universal functional F as

$$F(\rho) = \inf_{\substack{\psi \in \mathcal{Q} \\ \int_X |\psi|^2 = 1 \\ \rho_\psi = \rho}} (\psi, H_0 \psi), \quad (6)$$

where H_0 is the Hamiltonian (2) with the external potential $v \equiv 0$, we can write the energy variational principle (3) compactly as

$$E[v] = \inf_{\rho \in \mathcal{I}_N} \left\{ F(\rho) + \int_{\mathbb{R}^d} v \rho \right\}. \quad (7)$$

The explicit form of the universal functional is not currently known, despite several significant efforts towards that end. Several approximations have been put forth, as noted in the introductory remarks, but none of them are entirely satisfactory. The largest errors for a purely density based approach—OFDFT—are associated with the kinetic energy component of $F(\rho)$. Kohn and Sham [KS65] introduced a practical workaround by introducing a fictitious non-interacting system of electrons for which the kinetic energy can be compute exactly. In practice, this covers a significant fraction of the kinetic energy component of the universal functional. To state this clearly, we define a space of N one-electron orbitals that yield a specified density ρ as

$$\mathcal{Q}_\rho^+ = \{(\phi_1, \phi_2, \dots, \phi_N) \in H^1(\mathbb{R}^d \times \mathbb{Z}_q; \mathbb{C}^N) : (\phi_i, \phi_j)_{L^2} = \delta_{ij}, |\phi_1|^2 + |\phi_2|^2 + \dots + |\phi_N|^2 = \rho\}. \quad (8)$$

It was shown in [Lie83] that \mathcal{Q}_ρ^+ is non-empty for every N -representable density $\rho \in \mathcal{I}_N$. Kohn and Sham decomposed the universal functional into three terms,

$$F(\rho) = T_{\text{KS}}(\rho) + U_{\text{H}}(\rho) + E_{\text{XC}}(\rho),$$

where the Kohn-Sham kinetic energy, which corresponds to kinetic energy of a non-interacting collection of electrons, is given by

$$T_{\text{KS}}(\rho) = \frac{1}{2} \min_{\mathcal{Q}_\rho^+} \sum_{i=1}^N \int_{\mathbb{R}^d \times \mathbb{Z}_q} \|\nabla \phi_i\|^2 dx_i, \quad (9)$$

and U_{H} and E_{XC} are the Hartree potential and the exchange correlation functional, respectively. It is to be noted that $T_{\text{KS}}(\rho)$ was originally formulated for ground-state densities, but the extension specified in equation (9) to N -representable densities is due to Lieb [Lie83]. However, since the Kohn-Sham approach relies on the fictitious orbitals $\{\phi_k\}_{k=1}^N$, its computational cost becomes prohibitive for large systems, prompting the development of orbital-free approaches that provide a direct approximation of $T_{\text{KS}}(\rho)$ for any N -representable $\rho \in \mathcal{I}_N$. This, as noted earlier, remains elusive.

The goal of the present work is to develop a new approach to computing $T_{\text{KS}}(\rho)$ for a much larger class of densities than \mathcal{I}_N exactly. This can be viewed as an algorithm to generate $(\rho, T_{\text{KS}}(\rho))$ pairs that can be used to learn a $\rho \mapsto T_{\text{KS}}(\rho)$ map for a much larger class of densities than is currently possible with DFT-based methods. For sake of simplicity, we restrict ourselves to spin-unpolarized where the electrons are paired in each orbital—thus, $\int_{\mathbb{R}^d} \rho = 2N$ for some $N \in \mathbb{N}$. We refer to systems as *Restricted Kohn-Sham* (RKS) systems, following [AC09]. In this case, the expression for the non-interacting kinetic energy simplifies to

$$T_{\text{RKS}}(\rho) = \min_{\mathcal{Q}_\rho^{++}} \sum_{i=1}^N \int_{\mathbb{R}^d} \|\nabla \phi_i\|^2, \quad (10)$$

where

$$\mathcal{Q}_\rho^{++} = \{(\phi_1, \phi_2, \dots, \phi_N) \in H^1(\mathbb{R}^d; \mathbb{R}^N) : (\phi_i, \phi_j)_{L^2(\mathbb{R}^d; \mathbb{R})} = \delta_{ij}, 2 \sum_{i=1}^N |\phi_i|^2 = \rho\}. \quad (11)$$

The rest of the paper is concerned with the restricted non-interacting kinetic energy functional T_{RKS} .

2.2. Non-interacting v -representable densities. Define a collection of orthonormal N orbitals, for some $N \in \mathbb{N}$, as

$$\mathcal{P}_N = \{\Phi = (\phi_1, \phi_2, \dots, \phi_N) \in H^1(\mathbb{R}^d; \mathbb{R}^N) : (\phi_i, \phi_j)_{L^2(\mathbb{R}^d)} = \delta_{ij}, 1 \leq i, j \leq N\}. \quad (12)$$

We single out a special collection of potentials V_N as follows:

$$V_N = \left\{ v \in Y^d : \exists \Phi^\circ \in \mathcal{P}_N \text{ s.t. } \Phi^\circ = \arg \inf_{\Phi \in \mathcal{P}_N} \sum_{i=1}^N \int_{\mathbb{R}^d} (\|\nabla \phi_i\|^2 + 2\phi_i^2 v) \right\}. \quad (13)$$

Thus, for each $v \in V_N$, we define

$$I^N(v) = \min_{\Phi \in \mathcal{P}_N} \sum_{i=1}^N \int_{\mathbb{R}^d} (\|\nabla \phi_i\|^2 + 2\phi_i^2 v) = \sum_{i=1}^N \int_{\mathbb{R}^d} (\|\nabla \phi_i^\circ\|^2 + 2(\phi_i^\circ)^2 v). \quad (14)$$

Following the original formulation given by [KS65], the Euler-Lagrange equations of the minimization problem (14) yields the following eigenvalue problem: for $1 \leq k \leq N$ and for every $w \in H^1(\mathbb{R}^d)$,

$$\frac{1}{2} \int_{\mathbb{R}^d} \nabla \phi_k^\circ \cdot \nabla w + \int_{\mathbb{R}^d} v \phi_k^\circ w = \sum_{i=1}^N A_{ki} \int_{\mathbb{R}^d} \phi_i w \quad (15)$$

The Lagrange multipliers A_{ki} , whose existence is known from Proposition B.1, can be arranged in the form of a real and symmetric matrix A of size $N \times N$. Diagonalizing A yields $A = P\Lambda P^T$, where Λ is a diagonal matrix whose diagonal elements contain the eigenvalues λ_i and P is the orthogonal matrix whose columns are the eigenvectors of A . Define $\psi_i = \sum_{j=1}^N P_{ji} \phi_j^\circ$ —it is easy to see that $\psi_1, \psi_2, \dots, \psi_N \in \mathcal{P}_N$. We can also express the orbitals $(\phi_i^\circ)_{i=1}^N$ in terms of the eigenvectors of A as $\phi_k^\circ = \sum_{j=1}^N P_{kj} \psi_j$. Substituting this into equation (15) yields, for every $1 \leq j \leq N$,

$$\frac{1}{2} \int_{\mathbb{R}^d} \nabla \psi_j \cdot \nabla w + \int_{\mathbb{R}^d} v \psi_j w = \lambda_j \int_{\mathbb{R}^d} \psi_j w.$$

Note that $(\psi_1, \psi_2, \dots, \psi_N)$ is also a minimizer of (14). This implies that the infimum of the spectrum of $-\frac{1}{2}\Delta + v$ is achieved in the sense of distributions, and that $(\psi_i)_{i=1}^N$ constitute the N eigenfunctions of $-\frac{1}{2}\Delta + v$. We call the minimizers $(\psi_i)_{i=1}^N$ as restricted Kohn-Sham orbitals. The orbital corresponding to the lowest eigenvalue will be referred to as the *lowest eigenvalue orbital*. Note that if the spectrum is degenerate there can be multiple lowest eigenvalue orbitals.

The ground state density ρ_v corresponding to a potential $v \in V_N$ is computed in terms of the restricted Kohn-Sham orbitals as $\rho_v = 2 \sum_{i=1}^N \psi_i^2$. Note that ρ_v is an N -representable density since $\rho_v \in \mathcal{I}_{2N}$. We call the collection of all such ground-state densities as *non-interacting v -representable densities*. A precise characterization of which subset of \mathcal{I}_N corresponds to non-interacting v -representable densities is unknown. Note that any ground state density computed using DFT is a non-interacting v -representable density. For future use, we note that the kinetic energy in this special case is computed as $T_{\text{RKS}}(\rho_v) = \sum_{i=1}^N \int_{\mathbb{R}^d} \|\nabla \psi_i\|^2$.

We also present a lemma that will be useful in the subsequent analysis:

Lemma 2.1. *A lowest eigenvalue orbital of $v \in V_N$ minimizes the energy functional*

$$\mathcal{E}(f) = \frac{1}{2} \int_{\mathbb{R}^d} \|\nabla f\|^2 + \int_{\mathbb{R}^d} v f^2$$

over $H^1(\mathbb{R}^d)$, subject to the normalization constraint $\|f\|_{L^2(\mathbb{R}^d)} = 1$. Furthermore, the modulus of any minimizer is also a minimizer and thus qualifies as a lowest eigenvalue orbital of v . In addition, if $v \in L^\infty(\mathbb{R}^d)$, then the lowest eigenvalue orbital is unique up to a change of sign and can be chosen to be strictly positive.

Proof. Let ψ_1 be a lowest eigenvalue RKS orbital of $v \in V_N$ and let λ_1 be the eigenvalue corresponding to ψ_1 . Then the infimum of the spectrum of the operator

$$-\frac{1}{2}\Delta + v,$$

in the sense of distributions, is attained by ψ_1 . Since $-\frac{1}{2}\Delta + v$ is self-adjoint, the min-max theorem [RS78] implies that

$$\frac{1}{2} \int_{\mathbb{R}^d} \|\nabla \psi_1\|^2 + \int_{\mathbb{R}^d} v \psi_1^2$$

is the minimum of $\mathcal{E}(f)$ over $H^1(\mathbb{R}^d)$ under the constraint $\|f\|_{L^2(\mathbb{R}^d)} = 1$. Note that $\mathcal{E}(\psi_1) = \mathcal{E}(|\psi_1|) = \lambda_1$ and $|\psi_1|$ belong to the minimizing set. Therefore $|\psi_1|$ satisfies the following Euler-Lagrange equation:

$$\frac{1}{2} \int_{\mathbb{R}^d} \nabla |\psi_1| \cdot \nabla w + \int_{\mathbb{R}^d} v |\psi_1| w = \lambda_1 \int_{\mathbb{R}^d} |\psi_1| w,$$

for all $w \in H^1(\mathbb{R}^d)$, thereby showing that $|\psi_1|$ is also the lowest eigenvalue orbital. The final claim follows from Proposition B.2. \square

3. A VARIATIONAL PRINCIPLE FOR COMPUTING THE NON-INTERACTING KINETIC ENERGY

3.1. An informal introduction. As shown earlier in equation (10), the non-interacting kinetic energy functional can be formulated as a minimization problem over orthonormal functions whose squared moduli sum to a given N -representable electron density. Our approach to computing the non-interacting kinetic energy centers on an exact trigonometric reparametrization of the density in terms of *angle fields*. Informally, given a density ρ , we construct N orbitals $(\phi_k^\Theta)_{k=1}^N$ in terms of $N-1$ functions $\Theta = (\theta_l : \mathbb{R}^d \rightarrow [-\pi/2, \pi/2])_{l=1}^{N-1}$, which we refer to as angle fields, as follows:

$$\begin{aligned} \phi_N^\Theta &= \sqrt{\frac{\rho}{2}} \prod_{l=1}^{N-1} \cos \theta_l, \\ \phi_k^\Theta &= \sqrt{\frac{\rho}{2}} \sin \theta_k \prod_{l=1}^{k-1} \cos \theta_l, \quad k = 1, \dots, N-1. \end{aligned}$$

This parametrization addresses the following points:

- (i) The key constraint $2 \sum_{k=1}^N (\phi_k^\Theta)^2 = \rho$ in the minimization problem (10) is automatically satisfied. Without enforcing this constraint directly, one would need to introduce a Lagrange multiplier, leading to an adjoint problem and the possible complication of singular multipliers.¹
- (ii) This approach applies to *any* N -representable density and yields the energy explicitly, unlike Kohn–Sham DFT, which is restricted to non-interacting v -representable densities, whence there is no way of explicitly calculating energy for a given electron density.

¹In fact, the adjoint problem is not always well-posed, since it requires the Fréchet derivative of the constraint to be surjective; see Proposition B.1.

The specific reason for restricting the range of the angle fields to $[-\pi/2, \pi/2]$ is to remove discontinuities that can arise in the minimizer—a simple example is provided in Appendix A. A more rigorous argument in support of this range restriction will be provided below.

In terms of the trigonometric parametrization just introduced, the minimization problem for computing $T_{\text{RKS}}(\rho)$, for a non-interacting v -representable density, ρ , can be equivalently written as a minimization problem involving the angle fields as follows:

$$T_{\text{RKS}}(\rho) = \frac{1}{2} \inf_{\Theta} \int_{\mathbb{R}^d} \|\nabla \sqrt{\rho}\|^2 + \int_{\mathbb{R}^d} \rho \|\nabla \theta_1\|^2 + \int_{\mathbb{R}^d} \rho \left(\cos^2 \theta_1 \|\nabla \theta_2\|^2 + \cos^2 \theta_1 \cos^2 \theta_2 \|\nabla \theta_3\|^2 + \dots + \cos^2 \theta_1 \cos^2 \theta_2 \dots \cos^2 \theta_{N-2} \|\nabla \theta_{N-1}\|^2 \right).$$

The specific set over which Θ is minimized will be precisely defined later in this section.

We now present a detailed analysis of the foregoing sketch. For purposes of mathematical analysis, we first extend the definition of the non-interacting kinetic energy to a much larger class of densities than \mathcal{I}_{2N} , specifically densities ρ for which $\int_{\mathbb{R}^d} \rho$ is not an even integer. Note that this extension to $T_{\text{KS}}(\rho)$ remains well-defined even if intermediate densities obtained during an iterative algorithm are not N -representable.

3.2. Extension of the non-interacting kinetic energy functional. Recall that the functional $T_{\text{RKS}}(\rho)$ is defined for N -representable densities $\rho \in \mathcal{I}_N$ that integrate to an even integer. In the Kohn-Sham theory, it is computed on a much smaller subset of v -representable densities. As noted earlier, an explicit specification of the set of all v -representable densities is not available. In this work, we move in the opposite direction and generalize $T_{\text{RKS}}(\rho)$ to a much larger set than \mathcal{I}_{2N} . In particular, we extend it to include *pseudo-densities* which integrate to a non-integer value.

Following standard practice, we develop the formalism in terms of the square root of the electron density $u = \sqrt{\rho}$. We associate with any $u \in L^2(\mathbb{R}^d)$ a natural number N_u as follows:

$$N_u = \text{ceil} \left(\int_{\mathbb{R}^d} \frac{u^2}{2} \right). \quad (16)$$

Note that $N_u = 0$ if and only if $u = 0$ a.e. in \mathbb{R}^d .

Additionally, we associate with each $u \in H^1(\mathbb{R}^d)$, such that for $N_u \geq 1$, an *almost-orthonormal* set \mathcal{M}_u defined as

$$\mathcal{M}_u = \{(\phi_1, \phi_2, \dots, \phi_{N_u}) \in H^1(\mathbb{R}^d; \mathbb{R}^{N_u}) : (\phi_i, \phi_j)_{L^2(\mathbb{R}^d)} = 0, 1 \leq i, j \leq N_u, i \neq j, \|\phi_i\|_{L^2(\mathbb{R}^d)} = 1 \forall i \in [1, N_u - 1], 2 \sum_{i=1}^{N_u} |\phi_i|^2 = u^2\}. \quad (17)$$

Note that $\|\phi_{N_u}\|_{L^2(\mathbb{R}^d)}^2 = \int_{\mathbb{R}^d} u^2/2 - N_u + 1$, which is strictly positive and not equal to 1 unless $\int_{\mathbb{R}^d} u^2/2$ is an integer. In preparation for the extension of the non-interacting kinetic energy

functional, for all $u \in H^1(\mathbb{R}^d)$ such that $N_u \geq 1$, we define a functional $L : H^1(\mathbb{R}^d; \mathbb{R}^{N_u}) \rightarrow \mathbb{R}^+$ as

$$L(\phi_1, \phi_2, \dots, \phi_{N_u}) = \sum_{i=1}^{N_u} \int_{\mathbb{R}^d} \|\nabla \phi_i\|^2.$$

Lemma 3.1. *Let $u \in H^1(\mathbb{R}^d)$ such that $N_u \geq 1$. Then there exists $\Phi = (\phi_1, \dots, \phi_{N_u}) \in \mathcal{M}_u$ such that $L(\Phi) \leq C \int_{\mathbb{R}^d} \|\nabla u\|^2$ for some positive constant C that depends on N_u . Moreover, for any $\Phi \in \mathcal{M}_u$,*

$$\frac{1}{2} \int_{\mathbb{R}^d} \|\nabla u\|^2 \leq L(\Phi).$$

Proof. We show first that \mathcal{M}_u is non-empty and establish the upper bound on L . If $N_u = 1$, $\phi_1 = \frac{|u|}{\sqrt{2}}$ belongs to \mathcal{M}_u and upper bound on L is trivial. Suppose then that $N_u \geq 2$, and define $z = N_u - 1$ and $\alpha = 2z / \int_{\mathbb{R}^d} u^2$. Noting that $1/2 \leq \alpha < 1$, we define the function $g : \mathbb{R} \rightarrow \mathbb{R}$ as follows—see Figure 1:

$$g(x) = \begin{cases} \sqrt{\frac{1+\alpha}{2}} \cdot \frac{4(1+\alpha)}{3(1-\alpha)} \cdot x & \text{if } 0 \leq x < \frac{3(1-\alpha)}{4(1+\alpha)} \\ \sqrt{\frac{1+\alpha}{2}} & \text{if } \frac{3(1-\alpha)}{4(1+\alpha)} \leq x \leq 1 - \frac{3(1-\alpha)}{4(1+\alpha)} \\ \sqrt{\frac{1+\alpha}{2}} \cdot \frac{4(1+\alpha)}{3(1-\alpha)} \cdot (1-x) & \text{if } 1 - \frac{3(1-\alpha)}{4(1+\alpha)} < x \leq 1 \\ 0 & \text{otherwise} \end{cases}$$

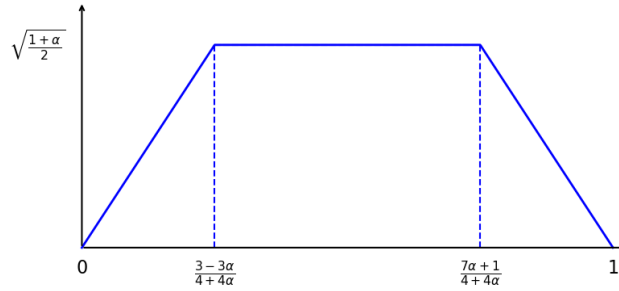


FIGURE 1. Plot of $g(x)$ over $[0, 1]$.

It is easy to see that $g \in H^1(\mathbb{R})$, $g^2 \leq \frac{1+\alpha}{2}$, $\int_0^1 g^2 = \alpha$ and g'^2 is bounded by a constant. Borrowing ideas from [MY58] and [Lie83], define, for $x = (x^1, \dots, x^d) \in \mathbb{R}^d$,

$$f(x^1) = \frac{2z \int_{-\infty}^{x^1} ds \int_{\mathbb{R}^{d-1}} dt \quad u^2(s, t)}{\int_{\mathbb{R}^d} u^2} - z.$$

Note that f is monotonically increasing from $-z$ to z . Defining

$$\begin{aligned}\phi^k(x) &= \frac{|u(x)|}{\sqrt{2}}(g(f(x^1) - k + 1) - g(f(x^1) + k)), \quad k = 1, \dots, N_u - 1, \\ \phi^{N_u}(x) &= \sqrt{\frac{u(x)^2}{2} - \sum_{k=1}^{N_u-1} |\phi^k(x)|^2},\end{aligned}\tag{18}$$

it follows that $\{\phi^k\}_{k=1}^{N_u-1}$ is an orthonormal set in $L^2(\mathbb{R}^d; \mathbb{R})$, $|\phi^k|^2 \leq \frac{1+\alpha}{2} \frac{u^2}{2}$ for all $1 \leq k \leq N_u - 1$, and $\sum_{k=1}^{N_u-1} |\phi^k|^2 \leq \frac{1+\alpha}{2} \frac{u^2}{2}$. Noting that $\phi^k/|u|$ is an odd function with respect to $f(x^1)$ whereas $\phi^{N_u}/|u|$ is even, it is evident that ϕ^{N_u} is orthogonal to all the elements of the above mentioned orthonormal set. Hence, $\Phi = (\phi^1, \phi^2, \dots, \phi^{N_u}) \in \mathcal{M}_u$, thereby establishing that \mathcal{M}_u is non-empty.

It is also easy to see that for $1 \leq k \leq N_u - 1$,

$$2\|\nabla\phi^k(x)\|^2 \leq \|\nabla u\|^2 + u(x)^2(g'(f(x^1) - k + 1) - g'(f(x^1) + k))^2 f'(x^1)^2.$$

Since g' is bounded by a constant, we get, following the proof in Theorem 1.2 of [Lie83], that

$$\sum_{k=1}^{N_u-1} \int_{\mathbb{R}^d} \|\nabla\phi^k(x)\|^2 \leq C_1 N_u^2 \int_{\mathbb{R}^d} \|\nabla u\|^2,$$

where $C_1 \geq 1$ is independent of u and d . We also have

$$2\phi^{N_u} \nabla \phi^{N_u} = u \nabla u - 2 \sum_{k=1}^{N_u-1} \phi^k \nabla \phi^k.$$

Note that $\frac{(1-\alpha)|u|}{4} \leq \phi^{N_u} \leq \frac{|u|}{2}$ and recall that $1/2 \leq \alpha < 1$. Using the Cauchy-Schwarz inequality, we get the following estimate:

$$\|\nabla \phi^{N_u}\|^2 \leq C_2 \left(\|\nabla u\|^2 + \sum_{k=1}^{N_u-1} \|\nabla \phi^k\|^2 \right)$$

where C_2 is independent of u and d , thus concluding the first part of the proof.

To prove the second part, note that for any $\Phi = (\phi_1, \phi_2, \dots, \phi_{N_u}) \in \mathcal{M}_u$, we have $\sum_{i=1}^{N_u} \phi_i^2 = \frac{u^2}{2}$. Taking the weak derivative on both sides and using the Cauchy-Schwarz inequality proves the second part of the proof. \square

Remark. *The upper bound in the foregoing lemma is not optimal with respect to N_u . However, optimal bounds were obtained in [ZM83] and [BG96].*

Remark. *Note that $\phi^{N_u} \geq 0$. This observation will be used later in a later section.*

The foregoing lemma shows that \mathcal{M}_u is non-empty, and that L is bounded from below. We can hence define $T : H^1(\mathbb{R}^d) \rightarrow \mathbb{R}_{\geq 0}$ such that

$$T(u) = \begin{cases} 0, & N_u = 0, \\ \inf_{\Phi \in \mathcal{M}_u} L(\Phi), & N_u \geq 1. \end{cases}\tag{19}$$

Theorem 3.2. *The infimum in equation (19) is achieved for any $u \in H^1(\mathbb{R}^d)$ with $N_u \geq 1$.*

Proof. Let $\Phi_i = (\phi_i^1, \phi_i^2, \dots, \phi_i^{N_u})$ be a minimizing sequence for $\inf_{\Phi \in \mathcal{M}_u} L(\Phi)$. It follows from Lemma 3.1 that the sequences $\{\phi_i^k\}_{i=1}^\infty$ are bounded in $H^1(\mathbb{R}^d)$ for all $1 \leq k \leq N_u$. Hence ϕ_i^k converge along a common subsequence to some ϕ^k weakly in $H^1(\mathbb{R}^d)$. We get, using Theorem 3.3 in [Lie83], strong convergence in $L^2(\mathbb{R}^d)$ and hence pointwise almost everywhere in \mathbb{R}^d along a common subsequence, for all $1 \leq k \leq N_u$. For the sake of convenience we notate this subsequence with same subscript i . Using pointwise convergence, we see that $2 \sum_{k=1}^{N_u} (\phi^k)^2 = u^2$. Similarly, using dominated convergence theorem, we can establish that $(\phi^1, \phi^2, \dots, \phi^{N_u})$ is almost orthonormal since $|\phi_i^k| \leq |u|$ for all $1 \leq k \leq N_u$. It follows that $\Phi = (\phi^1, \phi^2, \dots, \phi^{N_u}) \in \mathcal{M}_u$. Using the weak limit we also have $\int_{\mathbb{R}^d} \|\nabla \phi^k\|^2 \leq \liminf_{i \rightarrow \infty} \int_{\mathbb{R}^d} \|\nabla \phi_i^k\|^2$, which concludes the proof. \square

This theorem show that there exists a minimizer $\Phi \in \mathcal{M}_u$ of L . We note that this is trivially true for all u such that $N_u = 1$, in which case, $T(u) = \frac{1}{2} \int_{\mathbb{R}^d} \|\nabla u\|^2$. Also note that $T(\sqrt{\rho}) = T_{\text{RKS}}(\rho)$ for every $\rho \in \mathcal{I}_{2N}$. This shows that T extends T_{RKS} for all densities with $\sqrt{\rho} \in H^1(\mathbb{R}^d)$. We work with T instead of T_{RKS} in what follows.

3.3. Minimization problem. Let $u \in H^1(\mathbb{R}^d)$ such that $N_u \geq 2$. For some $N \in \mathbb{N}$, let $\Theta = (\theta_1, \theta_2, \dots, \theta_{N-1}) \in L^1_{loc}(\mathbb{R}^d; \mathbb{R}^{N-1})$. Then, we first define following $N - 1$ functions:

$$u_k = \frac{|u|}{\sqrt{2}} \prod_{i=1}^{k-1} \cos \theta_i, \quad 1 \leq k < N.$$

Further, we construct a set of orbitals $(\varphi_k^{\Theta, u})_{k=1}^N$ as follows:

$$\begin{aligned} \varphi_N^{\Theta, u} &= u_{N-1} \cos \theta_{N-1} = \frac{|u|}{\sqrt{2}} \prod_{i=1}^{N-1} \cos \theta_i, \\ \varphi_k^{\Theta, u} &= u_k \sin \theta_k = \frac{|u|}{\sqrt{2}} \sin \theta_k \prod_{i=1}^{k-1} \cos \theta_i, \quad 1 \leq k \leq N-1. \end{aligned} \tag{20}$$

We will use the shorthand notation $\Phi^{\Theta, u} = (\varphi_1^{\Theta, u}, \varphi_2^{\Theta, u}, \dots, \varphi_N^{\Theta, u})$ wherever appropriate. As noted in the introductory remarks, the advantage with this parameterization is that these orbitals satisfy the following constraint exactly:

$$2 \sum_{i=1}^N |\varphi_i^{\Theta, u}|^2 = u^2.$$

We define a collection of angle fields as follows:

$$\mathcal{S}_u = \{(\theta_1, \theta_2, \dots, \theta_{N_u-1}) \in H^1_{loc}(\mathbb{R}^d; \mathbb{R}^{N_u-1}) : u_k \nabla \theta_k \in L^2(\mathbb{R}^d; \mathbb{R}^3), 1 \leq k \leq N_u - 1\}. \tag{21}$$

It follows that $\Theta \in \mathcal{S}_u$ implies $\varphi_k^{\Theta,u}$ belong to $H^1(\mathbb{R}^d)$ for all $1 \leq k \leq N_u$. Further, we define $\tilde{L} : \mathcal{S}_u \rightarrow \mathbb{R}^+$ as follows:

$$\tilde{L}(\Theta) = L(\Phi^{\Theta,u}) = \sum_{k=1}^{N_u} \int_{\mathbb{R}^d} \|\nabla \varphi_k^{\Theta,u}\|^2.$$

Using induction it follows that

$$\begin{aligned} \tilde{L}(\Theta) = & \frac{1}{2} \int_{\mathbb{R}^d} \|\nabla u\|^2 + \frac{1}{2} \int_{\mathbb{R}^d} u^2 \|\nabla \theta_1\|^2 + \frac{1}{2} \int_{\mathbb{R}^d} u^2 \left(\cos^2 \theta_1 \|\nabla \theta_2\|^2 \right. \\ & \left. + \cos^2 \theta_1 \cos^2 \theta_2 \|\nabla \theta_3\|^2 + \dots + \cos^2 \theta_1 \cos^2 \theta_2 \dots \cos^2 \theta_{N_u-2} \|\nabla \theta_{N_u-1}\|^2 \right). \end{aligned}$$

We define next a collection of angle fields that correspond to almost orthonormal orbitals:

$$\begin{aligned} \mathcal{A}_u = \{ \Theta \in L^1_{loc}(\mathbb{R}^d; \mathbb{R}^{N_u-1}) : & \langle \varphi_i^{\Theta,u}, \varphi_j^{\Theta,u} \rangle_{L^2(\mathbb{R}^d, \mathbb{R})} = 0, 1 \leq i < j \leq N_u, \\ & \|\varphi_i^{\Theta,u}\|_{L^2(\mathbb{R}^d)} = 1, 1 \leq i < N_u \}. \end{aligned}$$

Lemma 3.3. *Let $u \in H^1(\mathbb{R}^d)$ with $N_u \geq 2$. Then $\mathcal{S}_u \cap \mathcal{A}_u$ is non-empty.*

Proof. For all $1 \leq j < N_u$ define

$$\theta_j = \arcsin(g(f(x^1) - k + 1) - g(f(x^1) + k))$$

using Lemma 3.1. Note that $\text{supp}(\theta_i) \cap \text{supp}(\theta_j)$ has zero measure when $i \neq j$. It is then easy to see that $\Theta \in \mathcal{S}_u$ since $0 < \cos \sqrt{\frac{1+\alpha}{2}} \cos \theta_i \leq 1$. Further note that $\phi_k^{\Theta,u} = \phi_k$, with ϕ_k 's defined as in Lemma 3.1. Hence $\Theta \in \mathcal{A}_u$. \square

This lemma establishes that for every $\Theta \in \mathcal{S}_u \cap \mathcal{A}_u$, there exists a corresponding $\Phi^{\Theta,u} \in \mathcal{M}_u$. However, it is not necessarily true that for every $\Phi \in \mathcal{M}_u$ there exists a $\Theta \in \mathcal{S}_u \cap \mathcal{A}_u$ such that $\Phi^{\Theta,u} = \Phi$. Attempting to define Θ pointwise in order to satisfy this equality leads to two difficulties. First, $\arcsin(\phi/u)$ can be discontinuous even when ϕ itself is continuous. Second, using the atan2 function to determine θ_{N_u-1} from the ratio of $\phi_{N_u-1}^{\Theta,u}$ and $\phi_{N_u}^{\Theta,u}$ will also yield discontinuity. Explicit counterexamples for both situations are provided in Appendix A. This implies that we cannot replace minimization over Φ with one over $\Phi^{\Theta,u}$. To resolve this issue, we start by defining

$$\mathcal{M}_u^+ = \{ \Phi = (\phi_1, \phi_2, \dots, \phi_{N_u}) \in \mathcal{M}_u : \phi_{N_u} \geq 0 \}. \quad (22)$$

As remarked in Lemma 3.1, the set \mathcal{M}_u^+ is also non-empty. Following the same reasoning as in Theorem 3.2 we define

$$T^+(u) = \min_{\Phi \in \mathcal{M}_u^+} L(\Phi). \quad (23)$$

Since $\mathcal{M}_u^+ \subset \mathcal{M}_u$, it holds that $T(u) \leq T^+(u)$. Further, using Lemma 2.1 it follows that $T(u) = T^+(u)$ when u^2 is a non-interacting v -representable ground state density. We resolve the issues raised earlier in this section by recourse to the following theorem.

Theorem 3.4. *Let $u \in H^1(\mathbb{R}^d)$ with $N_u \geq 2$ and define a subset of \mathcal{S}_u as follows:*

$$\mathcal{S}_u^+ = \{ \Theta \in \mathcal{S}_u : |\theta_i| \leq \pi/2, 1 \leq i < N_u \}.$$

Then,

$$T^+(u) = \lim_{\delta \downarrow 0^+} \min_{\Theta \in \mathcal{S}_u^+ \cap \mathcal{A}_u^\delta} \tilde{L}(\Theta), \quad (24)$$

where, for every $\delta > 0$,

$$\mathcal{A}_u^\delta = \left\{ \Theta \in L_{loc}^1(\mathbb{R}^d; \mathbb{R}^{N_u-1}) : \left| \langle \varphi_i^{\Theta, u}, \varphi_j^{\Theta, u} \rangle_{L^2(\mathbb{R}^d, \mathbb{R})} \right| \leq \delta, 1 \leq i < j \leq N_u, \right. \\ \left. \left\| \varphi_i^{\Theta, u} \right\|_{L^2(\mathbb{R}^d)} - 1 \leq \delta, 1 \leq i < N_u \right\}.$$

Proof. The proof is split into two parts. In the first part, we show that there exists a sequence $\{\Theta_\epsilon\}$ in \mathcal{S}_u^+ such that $\tilde{L}(\Theta_\epsilon)$ converges to $T^+(u)$. Later we show that a subsequence of the original sequence belongs to \mathcal{A}_u^δ and conclude the proof of the theorem.

We begin by noting that since $u \neq 0$ a.e., $\sup |u| > 0$. However, $\inf |u| = 0$ because $u \in L^2(\mathbb{R}^d)$. This can cause trouble for weak differentiability when dealing with division by u . To resolve this, we let $\Phi = (\phi_1, \phi_2, \dots, \phi_{N_u}) \in \mathcal{M}_u^+$ be such that $T^+(u) = L(\Phi)$. For $1 > \epsilon_1 > 0$ define $u_{1, \epsilon_1} = \frac{|u|}{\sqrt{2}}$ and

$$h_{1, \epsilon_1} = \frac{\phi_1}{u_{1, \epsilon_1} + \epsilon_1}.$$

Recall that $\phi_1^2 \leq u_{1, \epsilon_1}^2$, and $\phi_1 \in H^1(\mathbb{R}^d)$. Therefore, h_{1, ϵ_1} is strictly bounded by 1 and belongs to $H_{loc}^1(\mathbb{R}^d)$. Hence, defining $\theta_{1, \epsilon_1} = \sin^{-1}(h_{1, \epsilon_1})$, we see that $|\theta_{1, \epsilon_1}| < \frac{\pi}{2}$ and θ_{1, ϵ_1} is weakly differentiable. We recursively define, for $1 \leq k \leq N_u - 1$ and $1 > \epsilon_k > 0$,

$$u_{k, \epsilon_k} = \frac{|u|}{\sqrt{2}} \prod_{i=1}^{k-1} \cos \theta_{i, \epsilon_i}, \quad h_{k, \epsilon_k} = \frac{\phi_k}{u_{k, \epsilon_k} + \epsilon_k}, \quad \theta_{k, \epsilon_k} = \sin^{-1}(h_{k, \epsilon_k}). \quad (25)$$

For $1 \leq k \leq N_u - 1$ we have

$$2\phi_k^2 \leq u^2 - 2 \sum_{i=1}^{k-1} \phi_i^2, \quad \text{and} \quad u_{1, \epsilon_1}^2 - \sum_{i=1}^{k-1} u_{i, \epsilon_i}^2 \sin^2 \theta_{i, \epsilon_i} = u_{k, \epsilon_k}^2.$$

Using recursion we get $\phi_k^2 \leq u_{k, \epsilon_k}^2$, whence $|h_{k, \epsilon_k}| < 1$. Further, for $1 \leq k \leq N_u - 1$, we have $u_{k, \epsilon_k} \geq 0$ and $u_{k, \epsilon_k} = 0$ only when $u = 0$. Note that the inequalities shown above make all the functions well-defined. Similar to the case of θ_{1, ϵ_1} , it is easy to see that $|\theta_{k, \epsilon_k}| < \pi/2$ and θ_{k, ϵ_k} is weakly differentiable for $1 \leq k \leq N_u - 1$.

Since $\sin \theta_{k, \epsilon_k} = h_{k, \epsilon_k}$ and $\cos \theta_{k, \epsilon_k} = \sqrt{1 - h_{k, \epsilon_k}^2}$ for $1 \leq k \leq N_u - 1$, we have $\cos \theta_{k, \epsilon_k} \nabla \theta_{k, \epsilon_k} = \nabla h_{k, \epsilon_k}$, and $-\sin \theta_{k, \epsilon_k} \nabla \theta_{k, \epsilon_k} = \nabla \sqrt{1 - h_{k, \epsilon_k}^2}$, and hence that

$$\|\nabla \theta_{k, \epsilon_k}\|^2 = \|\nabla h_{k, \epsilon_k}\|^2 + \left\| \nabla \sqrt{1 - h_{k, \epsilon_k}^2} \right\|^2.$$

Noting that $u_{1, \epsilon_1} \in H^1(\mathbb{R}^d)$ we conclude that $\theta_{1, \epsilon_1} \in H_{loc}^1(\mathbb{R}^d)$ and $u_{1, \epsilon_1} \theta_{1, \epsilon_1} \in H^1(\mathbb{R}^d)$. Since $u_{k, \epsilon_k} = u_{k-1, \epsilon_{k-1}} \cos \theta_{k-1, \epsilon_{k-1}}$ we get, using a recursive argument, that both u_{k, ϵ_k} and $u_{k, \epsilon_k} \theta_{k, \epsilon_k}$ belongs to $H^1(\mathbb{R}^d)$ for all $1 \leq k \leq N_u - 1$. Moreover, $\theta_{k, \epsilon_k} \in H_{loc}^1(\mathbb{R}^d)$ for all $1 \leq k \leq N_u - 1$.

Let $\Theta_\epsilon = (\theta_{1,\epsilon_1}, \theta_{2,\epsilon_2}, \dots, \theta_{N_u-2,\epsilon_{N_u-2}}, \theta_{N_u-1,\epsilon_{N_u-1}})$ and note that $\Theta_\epsilon \in \mathcal{S}_u^+$. Then construct the corresponding set of orbitals $\Phi^{\Theta_\epsilon, u} = (\varphi_1^{\Theta_\epsilon, u}, \varphi_2^{\Theta_\epsilon, u}, \dots, \varphi_{N_u}^{\Theta_\epsilon, u})$. It is easy to see that $\varphi_k^{\Theta_\epsilon, u} = u_{k,\epsilon_k} \sin \theta_{k,\epsilon_k}$ for $1 \leq k \leq N_u - 1$. We thus have

$$\varphi_k^{\Theta_\epsilon, u} = \phi_k - \epsilon_k \sin \theta_{k,\epsilon_k}, \quad 1 \leq k \leq N_u - 1. \quad (26)$$

It follows that $\varphi_k^{\Theta_\epsilon, u}$ converges to ϕ_k pointwise almost everywhere and thus u_{k,ϵ_k} converges to $\sqrt{u^2/2 - \sum_{i=1}^{k-1} \phi_i^2}$ pointwise almost everywhere for $1 \leq k \leq N_u - 1$; note that $u_{1,\epsilon_1} = \frac{|u|}{\sqrt{2}}$. Further, using definition in equation (25), we also have

$$\varphi_k^{\Theta_\epsilon, u} = \left(\frac{u_{k,\epsilon_k}}{u_{k,\epsilon_k} + \epsilon_k} \right) \phi_k, \quad (27)$$

and thus,

$$\nabla \varphi_k^{\Theta_\epsilon, u} = \phi_k \nabla \left(\frac{u_{k,\epsilon_k}}{u_{k,\epsilon_k} + \epsilon_k} \right) + \left(\frac{u_{k,\epsilon_k}}{u_{k,\epsilon_k} + \epsilon_k} \right) \nabla \phi_k, \quad 1 \leq k \leq N_u - 1.$$

We introduce the following compact notation:

$$\lim_{\epsilon \rightarrow 0^+} = \lim_{\epsilon_1 \rightarrow 0^+} \lim_{\epsilon_2 \rightarrow 0^+} \dots \lim_{\epsilon_{N_u-2} \rightarrow 0^+} \lim_{\epsilon_{N_u-1} \rightarrow 0^+}.$$

If it holds that, for $1 \leq k \leq N_u - 1$,

$$\lim_{\epsilon \rightarrow 0^+} \int_{\mathbb{R}^d} \phi_k^2 \left\| \nabla \left(\frac{u_{k,\epsilon_k}}{u_{k,\epsilon_k} + \epsilon_k} \right) \right\|^2 = 0,$$

we then get

$$\lim_{\epsilon \rightarrow 0^+} \int_{\mathbb{R}^d} \left\| \nabla \varphi_k^{\Theta_\epsilon, u} \right\|^2 = \int_{\mathbb{R}^d} \left\| \nabla \phi_k \right\|^2, \quad (28)$$

using the Cauchy-Schwarz and the Dominated Convergence Theorem (DCT). Noting that

$$\phi_k^2 \left\| \nabla \left(\frac{u_{k,\epsilon_k}}{u_{k,\epsilon_k} + \epsilon_k} \right) \right\|^2 = \phi_k^2 \epsilon_k^2 \frac{\|\nabla u_{k,\epsilon_k}\|^2}{(u_{k,\epsilon_k} + \epsilon_k)^4},$$

and using the facts that $\phi_k^2 \leq (u_{k,\epsilon_k} + \epsilon_k)^2$ and $u_{k,\epsilon_k} \in H^1(\mathbb{R}^d)$, while not depending on ϵ_k , we get using DCT that

$$\lim_{\epsilon \rightarrow 0^+} \int_{\mathbb{R}^d} \phi_k^2 \left\| \nabla \frac{u_{k,\epsilon_k}}{u_{k,\epsilon_k} + \epsilon_k} \right\|^2 = 0, \quad 1 \leq k \leq N_u - 1.$$

Similarly, since $(\varphi_{N_u}^{\Theta_\epsilon, u})^2 = u_{1,\epsilon_1}^2 - \sum_{i=1}^{N_u-1} (\varphi_i^{\Theta_\epsilon, u})^2$, using equation (27) and Proposition B.3 it is easy to see that

$$\lim_{\epsilon \rightarrow 0^+} \int_{\mathbb{R}^d} \left\| \nabla \varphi_{N_u}^{\Theta_\epsilon, u} \right\|^2 = \int_{\mathbb{R}^d} \left\| \nabla \sqrt{u_{1,\epsilon_1}^2 - \sum_{i=1}^{N_u-1} \phi_i^2} \right\|^2.$$

Using

$$\phi_{N_u} = \sqrt{u_{1,\epsilon_1}^2 - \sum_{i=1}^{N_u-1} \phi_i^2}, \quad (29)$$

we get

$$\lim_{\epsilon \rightarrow 0^+} \int_{\mathbb{R}^d} \|\nabla \varphi_{N_u}^{\Theta_\epsilon, u}\|^2 = \int_{\mathbb{R}^d} \|\nabla \phi_{N_u}\|^2.$$

Further, using equation (28) we obtain

$$\lim_{\epsilon \rightarrow 0^+} \tilde{L}(\Theta_\epsilon) = T^+(u).$$

This concludes the first part of the proof.

The second part of the proof focuses on the orthonormality relation. Since, $|\varphi_i^{\Theta_\epsilon, u} \varphi_j^{\Theta_\epsilon, u}| < u^2/2$, we get using DCT that

$$\lim_{\epsilon \rightarrow 0^+} \int_{\mathbb{R}^d} \varphi_i^{\Theta_\epsilon, u} \varphi_j^{\Theta_\epsilon, u} = \int_{\mathbb{R}^d} \phi_i \phi_j, \quad 1 \leq i, j \leq N.$$

This implies that for every $\delta > 0$ there exists a sequence $\{\Theta_{\epsilon_j}\}_{j=1}^\infty \subset \mathcal{S}_u^+ \cap \mathcal{A}_u^\delta$ such that

$$\lim_{j \rightarrow \infty} \tilde{L}(\Theta_{\epsilon_j}) = T^+(u).$$

We therefore get

$$\inf_{\Theta \in \mathcal{S}_u^+ \cap \mathcal{A}_u^\delta} \tilde{L}(\Theta) \leq T^+(u). \quad (30)$$

Further, it is easy to see that there exists $\Theta_\delta \in \mathcal{S}_u^+ \cap \mathcal{A}_u^\delta$ such that $\varphi_k^{\Theta_\delta, u}$ is bounded in $H^1(\mathbb{R}^d)$ for all $1 \leq k \leq N_u$. Therefore, as $\delta \downarrow 0^+$, $\varphi_k^{\Theta_\delta, u}$ weakly convergence along a common subsequence in $H^1(\mathbb{R}^d)$ for all $1 \leq k \leq N_u$. Use the same argument as in Theorem 3.2 to see that $T^+(u) \leq \lim_{\delta \downarrow 0^+} \inf_{\Theta \in \mathcal{S}_u^+ \cap \mathcal{A}_u^\delta} \tilde{L}(\Theta)$.

Hence,

$$\lim_{\delta \downarrow 0^+} \inf_{\Theta \in \mathcal{S}_u^+ \cap \mathcal{A}_u^\delta} \tilde{L}(\Theta) = T^+(u),$$

thereby concluding the proof. \square

It is worth reiterating that \mathcal{M}_u^+ and \mathcal{A}_u^+ are introduced to avoid discontinuities of θ_{N_u} like the one shown in second part of Appendix A. Note that equation (29) would not be valid if we consider \mathcal{M}_u instead of \mathcal{M}_u^+ . Furthermore, to preserve the regularity of the angle fields, we approximate the orbitals. This results in an infimum problem rather than a true minimum and also causes a loss of exact orthonormality—we therefore work with the approximate orthonormality condition.

Since $T(u) = T^+(u)$ when u^2 is a non-interacting v -representable density and T^+ can be computed using the minimization problem (24), we use T^+ as a practical definition of the non-interacting kinetic energy functional.

Remark. In practice, $u \in H_0^1 \cap L^\infty(\Omega)$, where $\Omega \subseteq \mathbb{R}^d$ is open and bounded. Let Ω' be an open and bounded superset of Ω such that $\text{dist}(\Omega, \partial\Omega') > 0$. Using the fact that $C_c^\infty(\Omega')$ is dense in $H_0^1(\Omega')$ we get

$$T^+(u) = \lim_{\delta \downarrow 0^+} \inf \{ \tilde{L}(\Theta) : \Theta \in C_c^\infty(\Omega', [-\pi/2, \pi/2]^{N_u-1}) \cap \mathcal{A}_u^\delta \}.$$

This observation become particularly important for the numerical approximations presented in the next section since this permits us to approximate the angle fields using a smooth basis.

4. NUMERICAL EXAMPLES IN ONE DIMENSION

We present in this section a numerical demonstration of the ideas developed in this work. We restrict ourselves to the one-dimensional context and reserve a numerical study of the three-dimensional case for a future work. The primary goal of this numerical section is to demonstrate how the extension to $T_{\text{RKS}}(\rho)$ developed in this work can be computed for *any* N -representable ρ numerically. We wish to clarify that we do not attempt to provide a closed form expression for $T_{\text{RKS}}(\rho)$. We envisage this procedure to result in a sufficiently large dataset from which a suitable expression for $T_{\text{RKS}}(\rho)$ can be learned—we reserve this for a future work. Towards the end of this section, we consider densities which are not N -representable and show 1D slices of the extended non-interacting kinetic energy functional $T^+(\rho)$.

4.1. 1D optimization problem for non-interacting kinetic energy. Let $\rho \in H^1 \cap L^\infty(\mathbb{R})$ be a non-negative function compactly supported in $[0, 1]$ and let

$$N = \text{ceil} \left(\int_0^1 \frac{\rho}{2} \right).$$

We introduce the angle fields $\Theta = (\theta_1, \theta_2, \dots, \theta_{N-1}) \in H^1((0, 1))$ and solve the minimization problem (24) involving Θ by minimizing the following functional:

$$F(\Theta) = \frac{1}{2} \int_0^1 f(\Theta),$$

subject to the constraint

$$C_{ij}(\Theta) = \left| \int_0^1 \varphi_i^\Theta \varphi_j^\Theta - \delta_{ij} \right| < \delta, 1 \leq i, j \leq N, \text{ except for } i = j = N,$$

for some $\delta > 0$ and where

$$f(\Theta) = \rho(\theta'_1)^2 + \rho \left(\cos^2 \theta_1 (\theta'_2)^2 + \cos^2 \theta_1 \cos^2 \theta_2 (\theta'_3)^2 + \dots + \cos^2 \theta_1 \cos^2 \theta_2 \dots \cos^2 \theta_{N-2} (\theta'_{N-1})^2 \right).$$

Note that $T^+(\rho) = \lim_{\delta \downarrow 0^+} \frac{1}{2} \int_0^1 |(\sqrt{\rho})'|^2 + F(\Theta^{0,\delta})$ where $\Theta^{0,\delta}$ is the minimizer of F for a given δ .

Remark. The minimization problem (24) requires a two level minimization over δ . However, since $F(\Theta^{0,\delta})$ monotonically increases with as $\delta \downarrow 0^+$, for computational expediency, we fix δ to be machine precision as that is the best one could do numerically. Hence the constraints become $C_{ij} \approx 0$, Θ^0 is the minimizer of F with these constraints and $T^+(\rho) \approx \frac{1}{2} \int_0^1 |(\sqrt{\rho})'|^2 + F(\Theta)$. We later see that this approximation is very close to KSDFT results.

To solve this minimization problem, we approximate the angle fields using Radial Basis Functions (RBFs):

$$\theta_i(x) = \sum_{j=1}^M t_{ij} \sigma(|x - \xi_j|), \quad 1 \leq i < N,$$

where $\sigma : \mathbb{R}_+ \rightarrow \mathbb{R}$ is the parent RBF, $\{\xi_j\}_{j=1}^M$ are the centers of M nodes of the RBF approximation, and t_{ij} are the corresponding coefficients. We refer back to the final remark in Section 3.3 for validating the choice of the RBF approximation. We will use the shorthand notation σ_j in place of $\sigma(|\cdot - \xi_j|)$. For the results presented in this section, we choose the multiquadric RBF function $\sigma = \sqrt{1 + (x/\epsilon)^2}$, with $\epsilon = 0.1$. With this choice of approximation for Θ , both F and C are functions only of t_{ij} 's, and can be solved using any appropriate nonlinear programming algorithm. For the numerical result presented in this section, we used the Sequential Least Squares Quadratic Programming (SLSQP) method [Kra88] as implemented in the *SciPy* library². A listing of the various derivatives needed for a gradient-based minimization algorithm are provided in Appendix C.

For the local minimization problem using SLSQP, the choice of initial conditions plays a crucial role in determining the outcome of the optimization. Since SLSQP relies on local minimization, different initial conditions can lead to convergence towards different local minima, affecting the accuracy and consistency of the results. To account for this, we perform simulations using 100 randomly chosen initial conditions—the results are shown in Figure 2 as a log histogram of the computed energies for four randomly generated N -representable densities ρ , with $N = 3$. The dependence on the choice of initial conditions makes the theory algorithm-dependent in practice. We present in the next section a reliable choice of initial conditions to circumvent this issue.

4.2. Numerical Validation with KSDFT models. To validate our approach, we test it using a one-dimensional Kohn-Sham system confined to the interval $[0, 1]$. For a randomly generated 1D potential $v : [0, 1] \rightarrow \mathbb{R}$, we compute the first N eigenvalues and associated eigenvectors of the operator $-\frac{1}{2}\Delta + v$ on the domain $(0, 1)$ with Dirichlet boundary conditions. The non-interacting kinetic energy, T , of the system is then computed using equation (10). The electron density ρ is evaluated as twice the sum of the squares of the first N normalized eigenvectors. Finally, we evaluate the extended non-interacting kinetic energy T^+ using this density by solving the optimization problem presented in the previous section. We validate our method by checking that T^+ matches with the reference value T with high accuracy.

4.2.1. Special choice of initial condition. For the Kohn-Sham ground-state electron densities, we found that the initial conditions corresponding to the orbitals of a particle in a box produce results with desired accuracy among all the tested initial conditions. To illustrate this, we fix $N = 3$, discretize the domain into 1000 points, and set the number of radial basis functions (RBF) to 20. Figure 3 presents a log histogram showing the distribution of kinetic energies obtained from random initial conditions for four different densities ρ , generated from four

²<https://docs.scipy.org/doc/scipy/reference/generated/scipy.optimize.minimize.html>

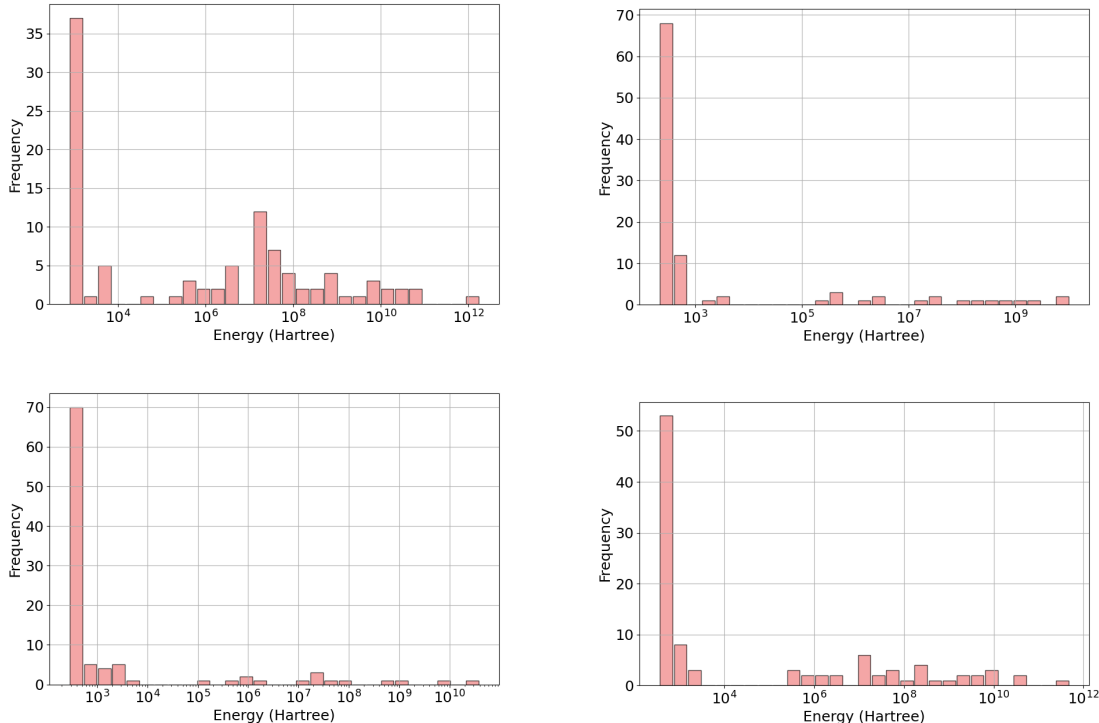


FIGURE 2. Histograms of non-interacting kinetic energy values, obtained from various initial conditions, for a given electron density, ρ , in each plot. Here, $\int_{\mathbb{R}} \rho = 2N = 6$.

randomly generated potentials. The special solution corresponding to an particles-in-a-box initial conditions are highlighted to illustrate their effectiveness in producing the best numerical solution. Figure 4 shows a zoomed-in view of the histograms in Figure 3, and, in particular, plots the histogram of the relative kinetic energy computed using our algorithm with respect to a Kohn-Sham calculation. It is evident that the particle-in-a-box initialization produces kinetic energies that are lower than those obtained from all other random initializations. We thus fix this special choice of initial conditions for all the simulations presented in the rest of this section. Note that this section focuses on demonstrating the effectiveness of the special initial condition rather than comparing with KS-DFT. Therefore, we have not used the optimal radial basis function or domain discretization.

4.2.2. *Comparison with Kohn-Sham models.* We now perform a detailed numerical comparison of the kinetic energies computed using the methods developed in this work and the standard Kohn-Sham model. We generate 500, 250, and 100 Kohn-Sham density samples for $N = 2, 3, 4$, respectively. For each case, different resolutions of the domain discretization (n_e) and numbers of radial basis functions (n_{rbf}) are employed to achieve desired accuracy. Figures 5, 6, and 7 demonstrate that the error between the computed kinetic energy and the Kohn-Sham solution, per electron, remains within 1 kcal/mol across these samples.

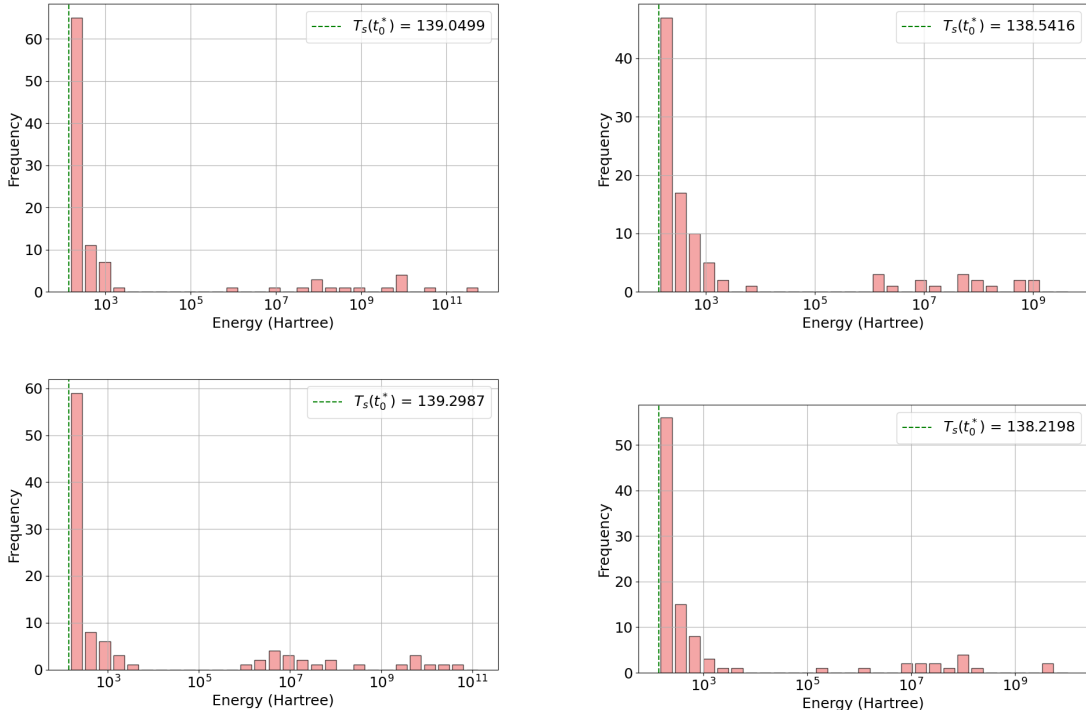


FIGURE 3. Histograms of non-interacting kinetic energy values, obtained from various initial conditions, for a given electron density, ρ , in each plot. Here, $\int_{\mathbb{R}} \rho = 2N = 6$ and t_0^* is initial condition obtained from the orbitals of particle in a box. The value $T_s(t_0^*)$, , representing the non-interacting kinetic energy evaluated using t_0^* , indicates that this particular choice of initial condition yields a kinetic energy close to the minimum.

4.2.3. *Computational Cost.* For each value of N , we also compute the average runtime and average total number of iterations required for SLSQP convergence. These results are summarized in Table 1, which indicates that the algorithm exhibits $\mathcal{O}(N^5)$ scaling. We emphasize that the goal of this work is not to develop a fast algorithm, but rather to demonstrate that the proposed approach for evaluating non-interacting kinetic energy is valid and produces results consistent with standard KSDFE calculations.

N	Avg. Iterations	Avg. Time (s)	Relative time
2	22	4.6	1
3	100	41	8.9
4	100	148	32.2

TABLE 1. Average SLSQP iterations and time for different values of N . The relative time refers to the time measured with respect to the average simulation time for $N = 2$.

4.2.4. *Rate of Convergence.* We generate 10 Kohn-Sham density samples for $N = 2, 3, 4$, maintaining the same domain discretization resolution (n_e) and number of radial basis functions

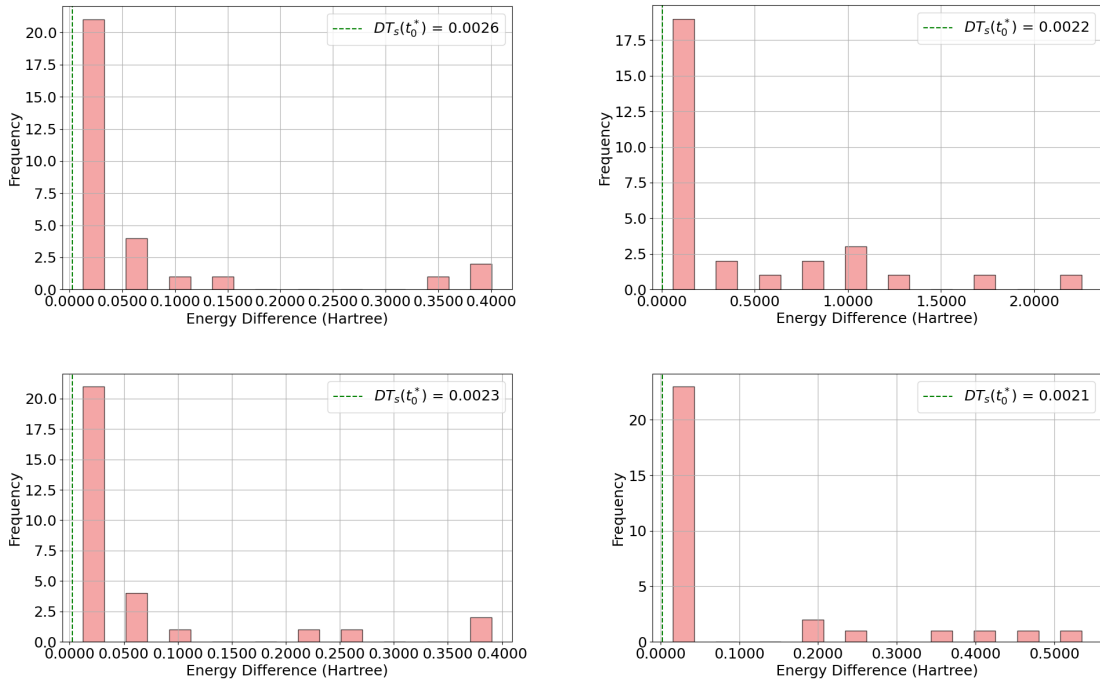


FIGURE 4. Histograms showing the lowest ten percent of non-interacting kinetic energy values, obtained from various initial conditions, relative to the non-interacting kinetic energy of the Kohn Sham system for a given electron density, ρ , in each plot. Here, $\int_{\mathbb{R}} \rho = 2N = 6$, t_0^* is initial condition obtained from the orbitals of particle in a box. The value $DT_s(t_0^*)$ is difference between non-interacting kinetic energy from the special initial condition and the non-interacting kinetic energy of the Kohn Sham system.

(n_{rbf}) as previously used to achieve desired accuracy in each case. This time, our goal is to examine the convergence rate of the SLSQP algorithm with respect to the iteration number when minimizing $F(\Theta)/2$ for each case. Figures 8, 9, and 10 illustrate the convergence behavior. We were not able to obtain a clear convergence order based on the results, but they are presented here for the sake of completeness.

4.3. A numerical studies of the properties of T^+ . The extended non-interacting kinetic energy T^+ was introduced in this work primarily for the sake of mathematical analysis. We present in this section some numerical simulations to investigate the convexity of T^+ . For this section, we use ρ instead of u as the primary variable of T^+ , but retain the functional symbol for notational convenience. Let ρ_1 and ρ_2 be two one-dimensional Kohn-Sham densities. We define a linear interpolation between them as $\rho_t = (1 - t)\rho_1 + t\rho_2$ for all $t \in [0, 1]$. Although $\sqrt{\rho_t} \in H^1(\mathbb{R})$, it may not necessarily be v -representable or N -representable. We analyze three cases: (i) $\int \rho_1 = \int \rho_2 = 2N$ for $N = 2, 3, 4$; (ii) $\int \rho_1 = 4$ and $\int \rho_2 = 6$; and (iii) $\int \rho_1 = 4$ and $\int \rho_2 = 8$. Results for the first case are shown in Figure 11, 12, and 13. These results provide numerical evidence for the convexity of the functional T^+ with respect to ρ on the convex set \mathcal{I}_{2N} for $N = 2, 3, 4$, respectively. This, however, does not establish convexity of T^+

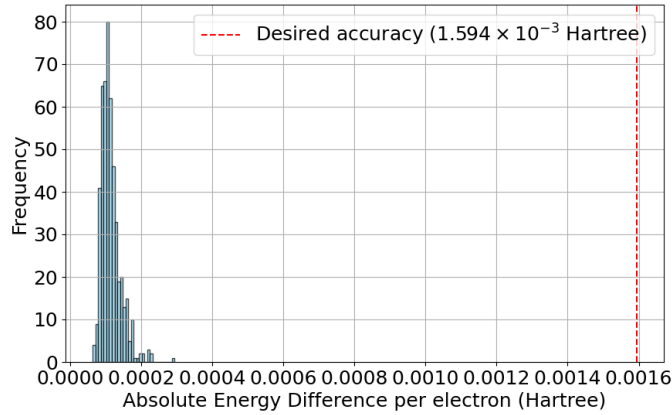


FIGURE 5. Error between the Kohn Sham non-interacting kinetic energy and non-interacting kinetic energy obtained from our minimisation method with special initial condition, per electron, for a given electron density, ρ , such that $\int_{\mathbb{R}} \rho = 2N = 4$. Here, $n_e = 1000$ and $n_{rbf} = 15$ is used.

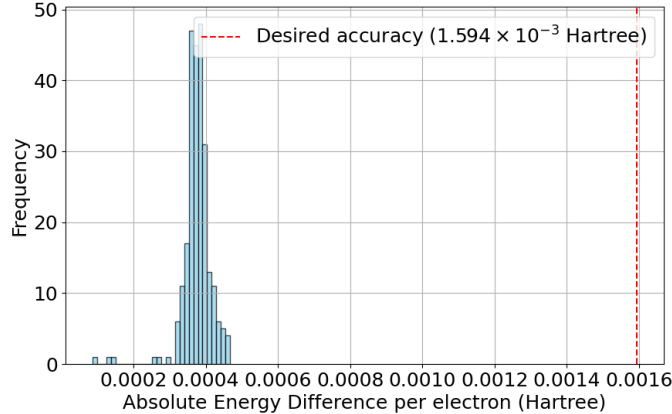


FIGURE 6. Error between the Kohn Sham non-interacting kinetic energy and non-interacting kinetic energy obtained from our minimisation method with special initial condition, per electron, for a given electron density, ρ , such that $\int_{\mathbb{R}} \rho = 2N = 6$. Here, $n_e = 1000$ and $n_{rbf} = 20$ is used.

by itself. Results for the second case are shown in Figure 14, illustrating concavity in direction from $\int \rho_t$ moving from 4 to 8. Finally, results for the third case are shown in Figure 15; a discontinuous jump around $\int \rho_t = 6$ occurs in this case. These results indicate that T^+ is not convex as a function of ρ , and is not in fact continuous, but when restricted to a fixed N , there is preliminary numerical evidence that it is convex over \mathcal{I}_{2N} .

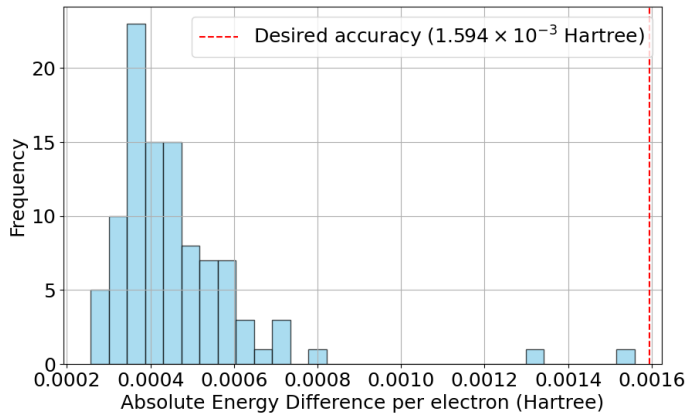


FIGURE 7. Error between the Kohn Sham non-interacting kinetic energy and non-interacting kinetic energy obtained from our minimisation method with special initial condition, per electron, for a given electron density, ρ , such that $\int_{\mathbb{R}} \rho = 2N = 8$. Here, $n_e = 2000$ and $n_{rbf} = 70$ is used.

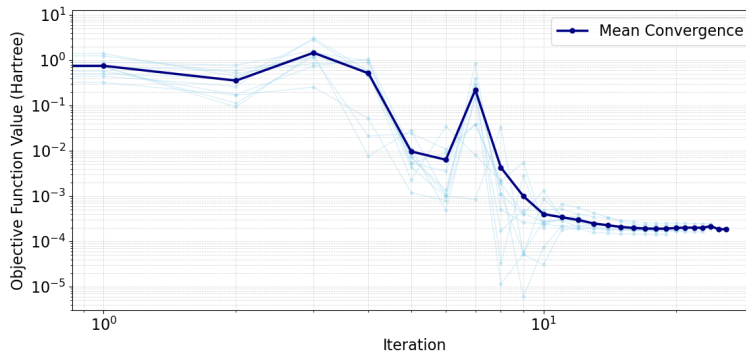


FIGURE 8. Rate of convergence of SLSQP for $N = 2$. Here $n_e = 1000$ and $n_{rbf} = 15$ is used.

5. DISCUSSION AND CONCLUSION

We analytically extended the restricted Kohn-Sham kinetic energy functional $T_{RKS}(\rho)$ to $T(u)$. We then established that the proposed functional $T^+(u)$ is an extension of $T(u)$. Specifically, we showed that $T^+(u) = T_{RKS}(u^2)$ when u corresponds to the ground-state square root electron density of the Kohn-Sham system.

The direct evaluation of $T_{RKS}(\rho)$ is delicate because the constraint $\rho = 2 \sum_i |\phi_i|^2$ must be enforced in the minimization. One natural way to enforce this constraint is through Lagrange multipliers. According to Lagrange multipliers on Banach spaces theorem (see Proposition B.1), existence of a multiplier requires that the Fréchet derivative of the constraint at the minimizer must be surjective. It is generally not possible to show surjectivity of the derivative for the constraint $\rho = 2 \sum_i |\phi_i|^2$ for an arbitrary ρ . When a multiplier does exist, it appears in the optimality condition through the adjoint of the derivative of the constraint, which leads

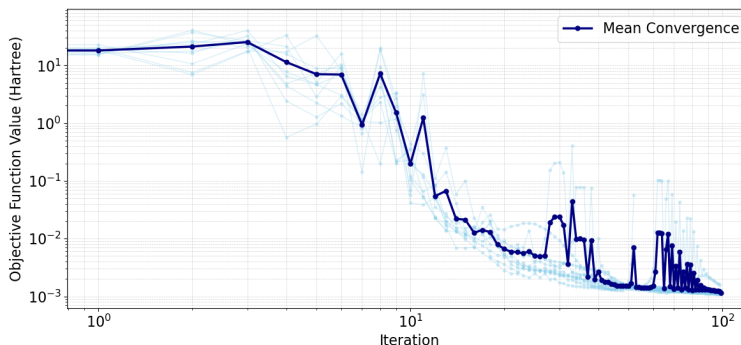


FIGURE 9. Rate of convergence of SLSQP for $N = 3$. Here $n_e = 1000$ and $n_{rbf} = 20$ is used.

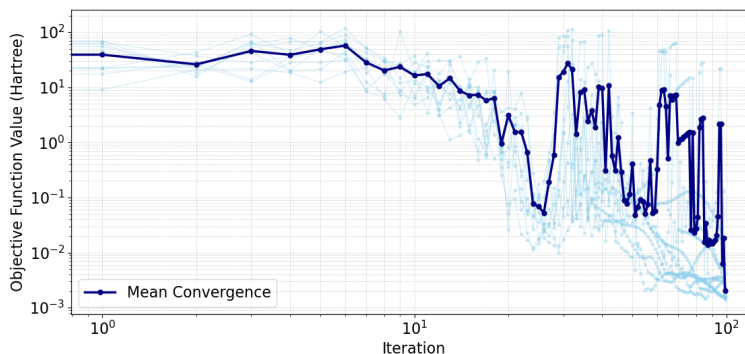


FIGURE 10. Rate of convergence of SLSQP for $N = 4$. Here $n_e = 2000$ and $n_{rbf} = 70$ is used.

to the corresponding adjoint problem. Moreover, even when a multiplier exists, it may be an unbounded function which could have its own numerical difficulties. Our parametrization avoids these issues by enforcing the constraint by construction, thereby eliminating the need to introduce and solve the adjoint problem explicitly. Our approach overcomes this issue by using a parametric representation that avoids the need to explicitly solve the adjoint problem. The primary contribution of this work is Theorem 3.4, where we show that the original minimization problem for the non-interacting kinetic energy is equivalent to a minimization problem involving angle fields that define the parametric representation referenced above.

The central limitation of the new approach presented here is the restriction to closed shell systems. The key advantage here is that the orbitals can be chosen to be real-valued, and this significantly simplifies the mathematical analysis. The extension to open shell systems requires a careful consideration of spin orbitals, and will be explored in a future work. An interesting observation in this regard is that the functional $T^+(\rho)$ introduced in this work provides a numerical value for the kinetic energy even $\int \rho$ is an odd integer. Though this value is not physically meaningful, it can be construed as an upper limit to the non-interacting kinetic energy of the corresponding open shell system.

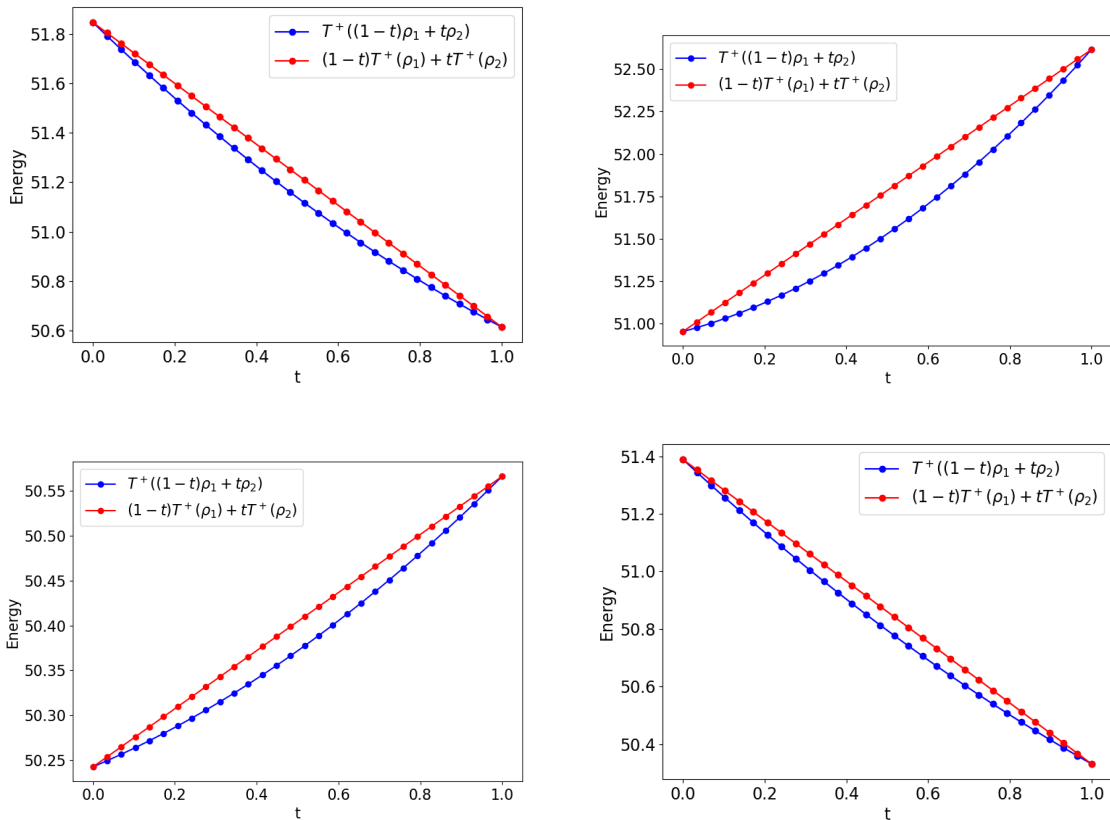


FIGURE 11. Comparison of $T^+((1-t)\rho_1 + t\rho_2)$ and $(1-t)T^+(\rho_1) + tT^+(\rho_2)$ when $\int_{\mathbb{R}} \rho_1 = \int_{\mathbb{R}} \rho_2 = 4$.

We solve the minimization problem for the non-interacting kinetic energy by approximating the angle fields using radial basis functions, and using a standard minimization algorithm—Sequential Least Squares Quadratic Programming (SLSQP)—with randomly generated initial conditions to solve the resulting finite dimensional optimization problem. We observed, in particular, that the initial conditions corresponding to the orbitals of a particle in a box consistently produced results with the lowest energy obtained from a set of randomly chosen initial conditions. The kinetic energy per electron computed using our algorithm were within 1 kcal/mol of the corresponding DFT calculations, demonstrating that our variational framework provides a reliable and accurate approach for computing the non-interacting kinetic energy functional.

We further examined the convexity properties of the proposed non-interacting kinetic energy functional—an analysis that, to the best of our knowledge, is not feasible with existing numerical methods. Within the convex set \mathcal{I}_N for fixed particle numbers $N = 2, 3, 4$, the functional appears to exhibit convex behavior. In contrast, concavity and/or discontinuities are observed when tested over densities with varying values of N .

The numerical demonstrations presented here are limited to one dimension, but the algorithm is readily generalizable to three dimensions—this will be pursued in a future work. The particular

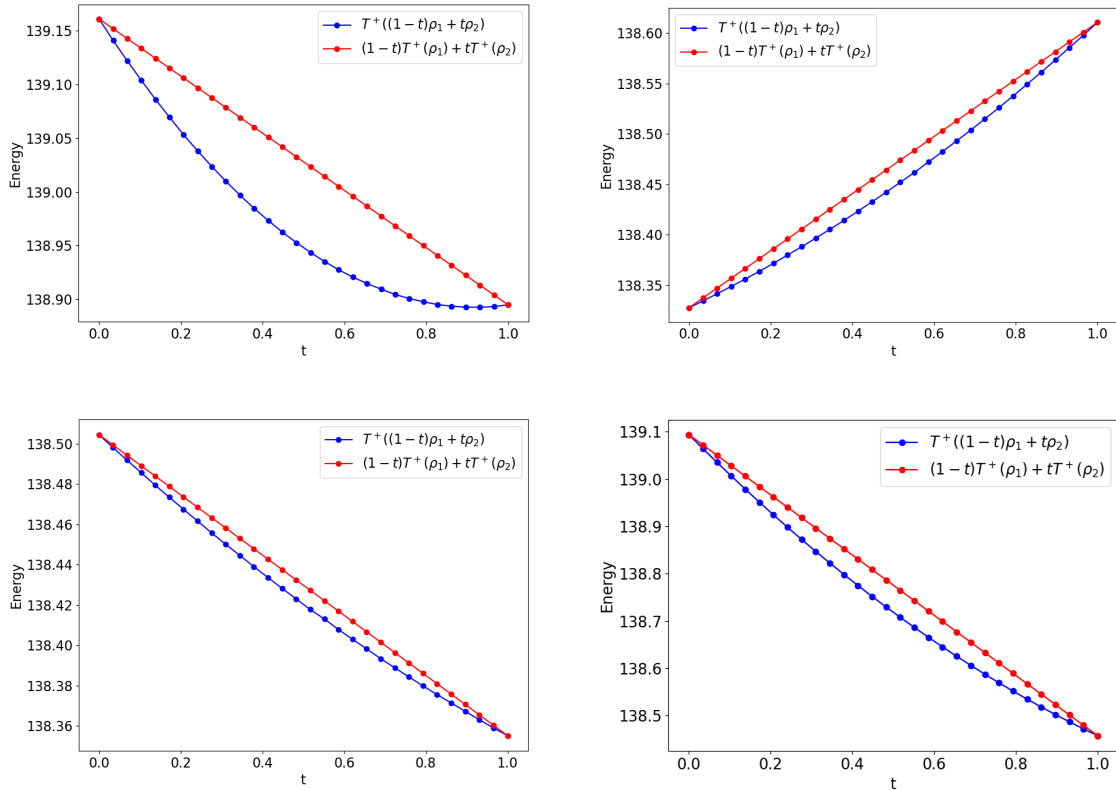


FIGURE 12. Comparison of $T^+((1-t)\rho_1 + t\rho_2)$ and $(1-t)T^+(\rho_1) + tT^+(\rho_2)$ when $\int_{\mathbb{R}} \rho_1 = \int_{\mathbb{R}} \rho_2 = 6$.

algorithm that we used in this work does not scale well with increasing N —this is another avenue for future improvements. Another major contribution of this work, however, is a new and reliable method to generate datasets consisting of pairs of densities and corresponding non-interacting kinetic energies without resorting to a Kohn-Sham system. Such a dataset is likely to provide a better starting point to create transferable machine learning models for the non-interacting kinetic energy functional since it provides greater control over the distribution of input densities ρ and allows for the generation of more diverse training data. Learning such a non-interacting kinetic energy, and implementing it within the context of an orbital-free density functional theory framework, will be pursued in the future.

ACKNOWLEDGMENTS

The authors gratefully acknowledge Vikram Gavini, Bikash Kanungo, and Sambit Das for stimulating discussions on DFT. They also thank the anonymous referees for their constructive comments and suggestions.

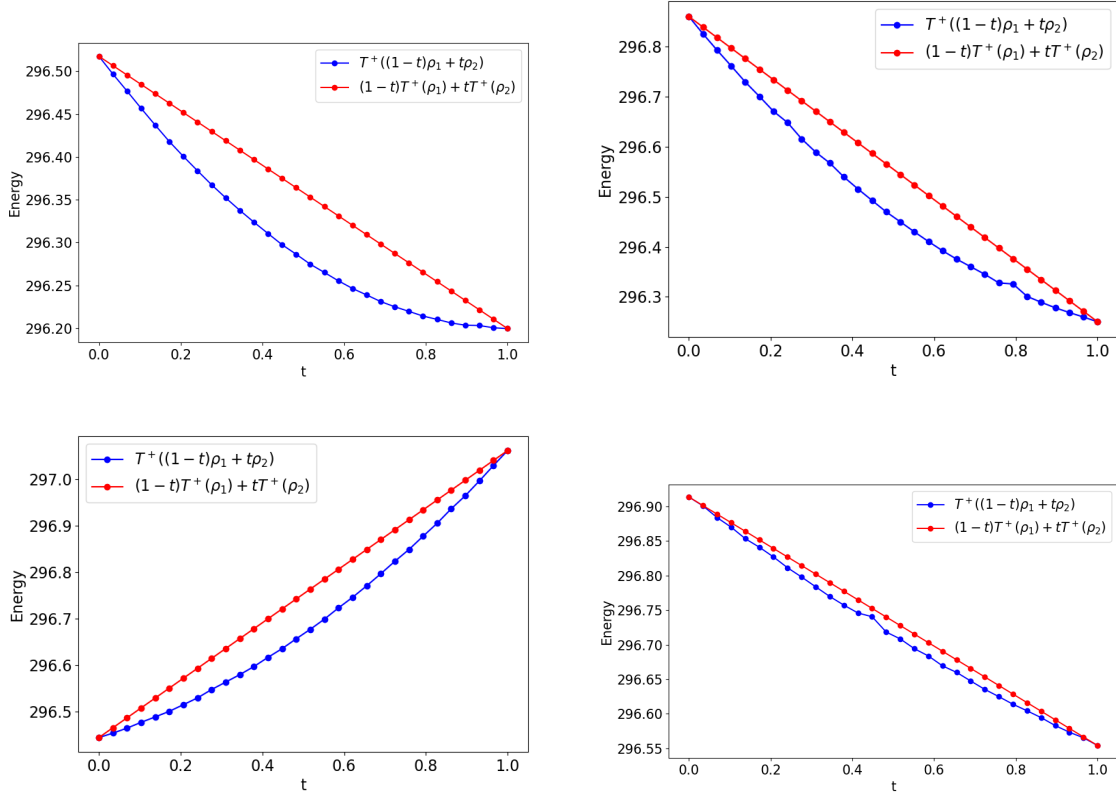


FIGURE 13. Comparison of $T^+((1-t)\rho_1 + t\rho_2)$ and $(1-t)T^+(\rho_1) + tT^+(\rho_2)$ when $\int_{\mathbb{R}} \rho_1 = \int_{\mathbb{R}} \rho_2 = 8$.

APPENDIX A. DISCONTINUITY OF ANGLE-FIELDS

A.1. Discontinuity during inversion. Let $w : \mathbb{R} \rightarrow \mathbb{R}$ be defined as

$$w(x) = |x|\eta(x), \quad (31)$$

where $\eta \in C_c^\infty(\mathbb{R})$ is a smooth cutoff with $\eta \equiv 1$ on $[-1/2, 1/2]$ and $\text{supp}(\eta) \subset [-1, 1]$. Then $w \in H^1(\mathbb{R})$, $w(0) = 0$, and $w \geq 0$. Define

$$\phi_1(x) = cw(x) \mathbf{1}_{[0, \infty)}(x), \quad \phi_2(x) = cw(x) \mathbf{1}_{(-\infty, 0]}(x), \quad (32)$$

with the normalization constant

$$c = \frac{1}{\sqrt{\int_0^\infty w(x)^2 dx}}. \quad (33)$$

By construction, $\phi_1, \phi_2 \in H^1(\mathbb{R})$ and $\phi_1, \phi_2 \geq 0$. Moreover,

$$\int_{\mathbb{R}} \phi_1(x)^2 dx = 1, \quad \int_{\mathbb{R}} \phi_2(x)^2 dx = 1, \quad \int_{\mathbb{R}} \phi_1(x)\phi_2(x) dx = 0. \quad (34)$$

Thus $\{\phi_1, \phi_2\}$ forms an orthonormal set in $L^2(\mathbb{R})$. Setting

$$u(x) = \sqrt{2\phi_1(x)^2 + 2\phi_2(x)^2} = cw(x), \quad (35)$$

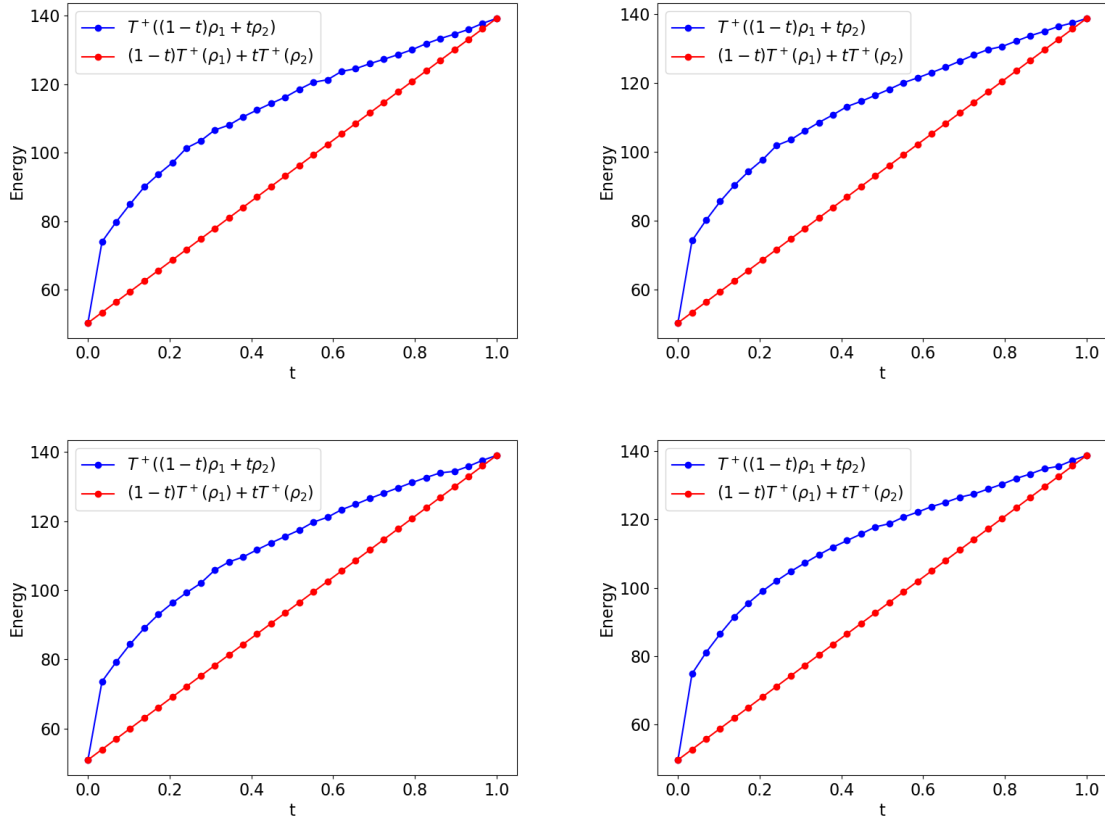


FIGURE 14. Comparison of $T^+((1-t)\rho_1 + t\rho_2)$ and $(1-t)T^+(\rho_1) + tT^+(\rho_2)$ when $\int_{\mathbb{R}} \rho_1 = 4$ and $\int_{\mathbb{R}} \rho_2 = 6$.

we may formally write

$$\phi_1(x) = \frac{u(x)}{\sqrt{2}} \sin(\theta(x)), \quad \phi_2(x) = \frac{u(x)}{\sqrt{2}} \cos(\theta(x)). \quad (36)$$

Note that $u \in H^1(\mathbb{R})$. Pointwise, the angle θ is determined as

$$\theta(x) = \begin{cases} 0, & x < 0, \\ \pi/2, & x > 0, \end{cases} \quad (37)$$

with any arbitrary value at $\theta(0)$. Hence θ has jump discontinuity at $x = 0$ and is not in $H_{loc}^1(\mathbb{R})$.

A.2. Discontinuity due to incompatibility. Let $\rho : [0, 1] \rightarrow \mathbb{R}$ be defined as

$$\rho(x) = 4(\sin^2(2\pi x) + \sin^2(3\pi x)). \quad (38)$$

Define the functions

$$\phi_1 = \sqrt{2} \sin(2\pi x), \quad \phi_2 = \sqrt{2} \sin(3\pi x), \quad (39)$$

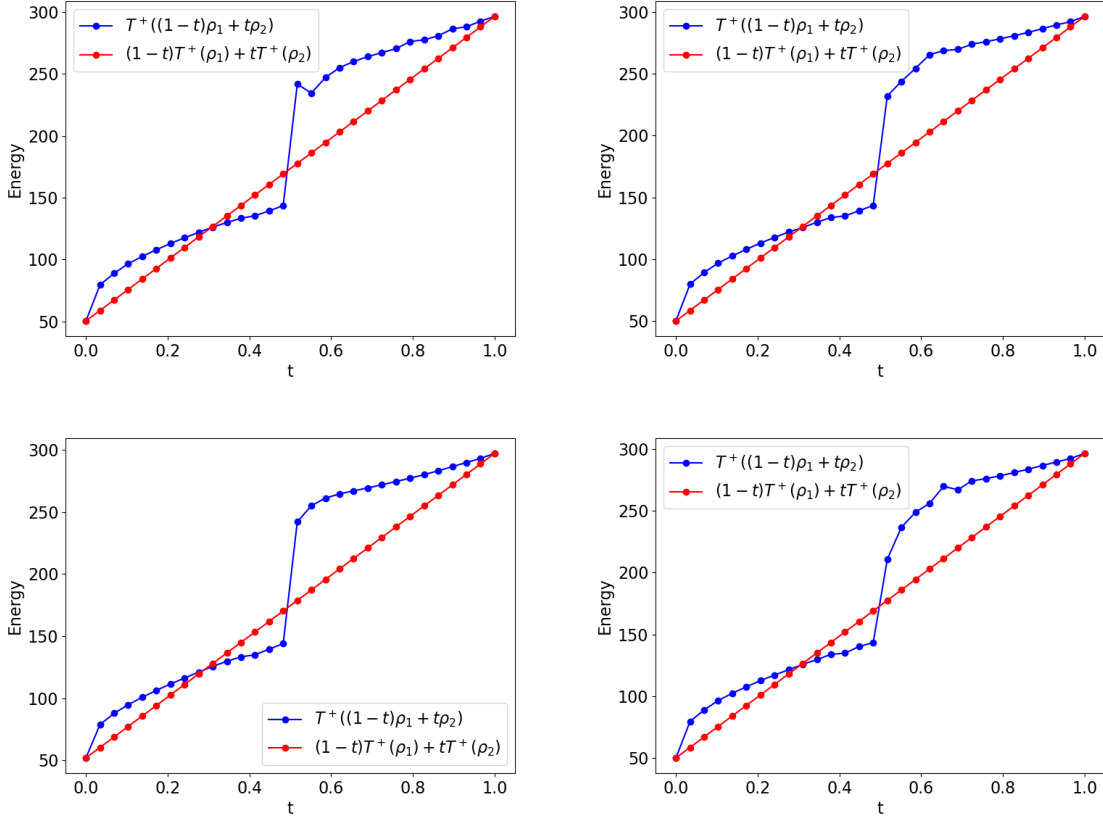


FIGURE 15. Comparison of $T^+((1-t)\rho_1 + t\rho_2)$ and $(1-t)T^+(\rho_1) + tT^+(\rho_2)$ when $\int_{\mathbb{R}} \rho_1 = 4$ and $\int_{\mathbb{R}} \rho_2 = 8$.

We observe that $\sqrt{\rho} \in H^1([0, 1])$, and similarly, $\phi_1, \phi_2 \in H^1([0, 1])$. Furthermore, ϕ_1 and ϕ_2 form an orthonormal set and $\phi_1^2 + \phi_2^2 = \rho/2$. Notice that

$$\phi_1 = \sqrt{\frac{\rho}{2}} \sin(\theta), \quad \phi_2 = \sqrt{\frac{\rho}{2}} \cos(\theta), \quad (40)$$

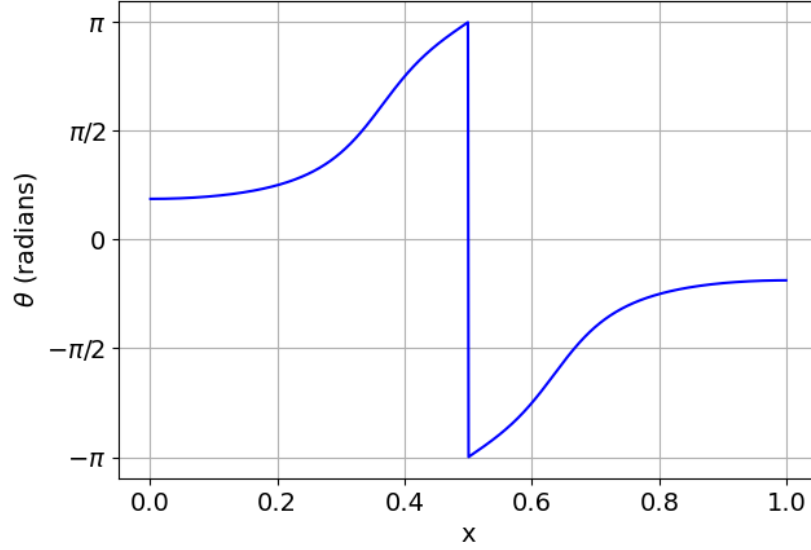
and hence that θ is uniquely determined using the atan2 function as

$$\theta = \text{atan2}(\phi_1, \phi_2). \quad (41)$$

A plot of $\theta(x)$ is shown in Figure 16. Observe that θ is uniquely defined but exhibits jump discontinuity. Consequently, θ is not weakly differentiable.

APPENDIX B. SUPPLEMENTARY PROPOSITIONS

Proposition B.1. [Section 4.14 in [Zei95]] *Let X and Y be real Banach spaces and U be an open subset of X . Let $f : U \rightarrow \mathbb{R}$ and $g : U \rightarrow Y$ be continuously Frechet differentiable functions. Suppose $u^* \in U$ is a local extremum of f subject to the constraint $g(x) = 0$. If the Frechet derivative $Dg(u^*) : X \rightarrow Y$ is a surjective linear map, then there exists a continuous*

FIGURE 16. Plot of $\theta(x)$ over $[0, 1]$ showing discontinuity.

linear functional $\lambda^* \in Y^*$, dual to the space Y , such that

$$Df(u^*) = \lambda \circ Dg(u^*),$$

where $Df(u^*) : X \rightarrow \mathbb{R}$ is Frechet derivative of f at u^* .

Proposition B.2. [Theorem 11.8 in [LL01]] Let $V \in L^1_{loc}(\mathbb{R}^d)$, $\psi_0 \in H^1(\mathbb{R}^d)$ be a minimizer of $\mathcal{E}(f) = \int_{\mathbb{R}^d} \|\nabla f\|^2 + \int_{\mathbb{R}^d} V f^2$ over $H^1(\mathbb{R}^d)$ with constraint $\|f\|_{L^2(\mathbb{R}^d)} = 1$, and $V|\psi_0|^2$ be summable. If $V_+ \in L^\infty(\mathbb{R}^d)$, then ψ_0 is unique up to sign change and can be chosen to be strictly positive.

Proposition B.3. [Theorem 6.9 in [LL01]] Let $f \in H^1(\mathbb{R}^d)$ and let $B = f^{-1}(\{0\})$. Then $\nabla f = 0$ for almost every $x \in B$.

APPENDIX C. GRADIENTS FOR THE RBF APPROXIMATION

The derivatives required for a gradient-based optimization algorithm are provided below for quick reference:

$$\begin{aligned} \frac{\partial F}{\partial t_{ij}} &= \int_0^1 h \sigma_j - (\rho \cos^2 \theta_1 \cos \theta_2^2 \dots \cos \theta_{i-1}^2 \theta'_i) \sigma'_j, \\ h &= \rho \cos^2 \theta_1 \dots \cos \theta_{i-1}^2 \cos \theta_i \sin \theta_i \\ &\quad \left((\theta'_{i+1})^2 + \cos^2 \theta_{i+1} (\theta'_{i+2})^2 + \dots + \cos^2 \theta_{i+1} \dots \cos^2 \theta_{N-2} (\theta'_{N-1})^2 \right), \\ \frac{\partial C_{kl}}{\partial t_{ij}} &= \frac{\partial D_{kl}}{\partial t_{ij}} + \frac{\partial D_{lk}}{\partial t_{ij}}, \\ \frac{\partial D_{kl}}{\partial t_{ij}} &= \int_0^1 g_{ik}(\Theta) \sigma_j \varphi_l^\Theta. \end{aligned}$$

In the final equation shown above, it is important to note that:

$$\frac{\partial \varphi_k^\Theta}{\partial t_{ij}} = g_{ik}(\Theta) \sigma_j,$$

where the following conditions hold, for $1 \leq k \leq N - 1$:

- When $k < i$, $g_{ik}(\Theta) = 0$,
- When $k = i$, we have

$$g_{ik}(\Theta) = \sqrt{\frac{\rho}{2}} \prod_{m=1}^k \cos(\theta_m),$$

- When $k > i$, we have

$$g_{ik}(\Theta) = -\sqrt{\frac{\rho}{2}} \sin(\theta_i) \sin(\theta_k) \prod_{m=1}^{i-1} \cos(\theta_m) \prod_{p=i+1}^{k-1} \cos(\theta_p).$$

Finally, when $k = N$, we have

$$g_{iN}(\Theta) = -\sqrt{\frac{\rho}{2}} \sin(\theta_i) \prod_{m=1}^{i-1} \cos(\theta_m) \prod_{p=i+1}^{N-1} \cos(\theta_p).$$

REFERENCES

- [AC09] A. Anantharaman and E. Cancès, *Existence of minimizers for kohn–sham models in quantum chemistry*, Annales de l’Institut Henri Poincaré C, Analyse non linéaire **26** (2009), no. 6, 2425–2455.
- [BG96] O. Bokanowski and B. Grebert, *A decomposition theorem for wave functions in molecular quantum chemistry*, Mathematical Models and Methods in Applied Sciences **06** (1996), no. 04, 437–466.
- [Cor25] T. C. Corso, *A rigorous formulation of density functional theory for spinless electrons in one dimension*, arXiv preprint (2025).
- [Fer27] E. Fermi, *Un metodo statistico per la determinazione di alcune priorieta del atomo*, Rend. Accad. Nat. Lincei **6** (1927), 602–607.
- [HBL25] Michael F. Herbst, Vejbjørn H. Bakkestuen, and Andre Laestadius, *Kohn–sham inversion with mathematical guarantees*, Phys. Rev. B **111** (2025), 205143.
- [HK64] P. Hohenberg and W. Kohn, *Inhomogeneous electron gas*, Phys. Rev. **136** (1964), B864–B871.
- [KLL+23] N. Kovachki, Z. Li, B. Liu, K. Azizzadenesheli, K. Bhattacharya, A. M. Stuart, and A. Anandkumar, *Neural operator: Learning maps between function spaces*, Journal of Machine Learning Research **24** (2023), 1–97.
- [Kra88] Dieter Kraft, *A software package for sequential quadratic programming*, DFVLR-Forschungsbericht DFVLR-FB 88-28, Deutsches Zentrum für Luft- und Raumfahrt (DLR), Oberpfaffenhofen, Germany, 1988.
- [KS65] W. Kohn and L. J. Sham, *Self-consistent equations including exchange and correlation effects*, Phys. Rev. **140** (1965), A1133–A1138.
- [Lev79] M. Levy, *Universal variational functionals of electron densities, first-order density matrices, and natural spin-orbitals and solution of the v-representability problem*, Proceedings of the National Academy of Sciences of the United States of America **76** (1979), no. 12, 6062–6065.
- [Lie83] E. H. Lieb, *Density functionals for coulomb systems*, Int. J. Quantum Chem. **24** (1983), 243–277.
- [LL01] Elliott H. Lieb and Michael Loss, *Analysis*, 2nd ed., Graduate Studies in Mathematics, vol. 14, American Mathematical Society, Providence, RI, 2001.

- [LLS23] M. Lewin, E. H. Lieb, and R. Seiringer, *Universal functionals in density functional theory*, pp. 115–182, Springer International Publishing, 2023.
- [MWH20] Ralf Meyer, Manuel Weichselbaum, and Andreas W. Hauser, *Machine learning approaches toward orbital-free density functional theory: Simultaneous training on the kinetic energy density functional and its functional derivative*, *Journal of Chemical Theory and Computation* **16** (2020), no. 9, 5685–5694, PMID: 32786898.
- [MY58] N. H. March and W. H. Young, *Variational methods based on the density matrix*, *Proceedings of the Physical Society* **72** (1958), no. 2, 182.
- [RS78] Michael Reed and Barry Simon, *Methods of modern mathematical physics. volume iv: Analysis of operators*, Academic Press, Academic Press, New York, 1978.
- [RWMT22] Kevin Ryczko, Sebastian J. Wetzol, Roger G. Melko, and Isaac Tamblyn, *Toward orbital-free density functional theory with small data sets and deep learning*, *Journal of Chemical Theory and Computation* **18** (2022), no. 2, 1122–1128, PMID: 34995061.
- [SPR+24a] S. M. Sutter, M. Penz, M. Ruggenthaler, R. van Leeuwen, and K. J. H. Giesbertz, *Solution of the v -representability problem on a one-dimensional torus*, *Journal of Physics A: Mathematical and Theoretical* **57** (2024).
- [SPR+24b] ———, *v -representability on a one-dimensional torus at elevated temperatures*, arXiv preprint (2024).
- [SRH+12] John C. Snyder, Matthias Rupp, Katja Hansen, Klaus-Robert Müller, and Kieron Burke, *Finding density functionals with machine learning*, *Phys. Rev. Lett.* **108** (2012), 253002.
- [Tho27] L.H. Thomas, *The calculation of atomic fields*, *Proc. Camb. Philos. Soc.* **23** (1927), 542–548.
- [WGC98] Y. A. Wang, N. Govind, and E. A. Carter, *Orbital-free kinetic-energy functionals for the nearly free electron gas*, *Physical Review B* **58** (1998), no. 20, 13465–13471.
- [Zei95] E. Zeidler, *Applied functional analysis: Main principles and their applications*, Applied Mathematical Sciences, vol. 109, Springer, New York, NY, 1995.
- [ZM83] G. Zumbach and K. Maschke, *New approach to the calculation of density functionals*, *Phys. Rev. A* **28** (1983), 544–554.